ELSEVIER

New insights into the southern margin of the Archean–Proterozoic boundary in the north-central United States based on U–Pb, Sm–Nd, and Ar–Ar geochronology

W.R. Van Schmus [a,*], D.A. Schneider [b], D.K. Holm [c], S. Dodson [b], B.K. Nelson [d]

[a] *Department of Geology, University of Kansas, Lawrence, KS 66045, USA*
[b] *Department of Geological Sciences, Ohio University, Athens, OH 45701, USA*
[c] *Department of Geology, Kent State University, Kent, OH 44242, USA*
[d] *Department of Geology, University of Washington, Seattle, WA 12345, USA*

Abstract

New geophysical analysis of the Precambrian basement in Minnesota–Iowa–Wisconsin indicates that an Archean–Proterozoic boundary (Spirit Lake trend) previously recognized in NW Iowa can be continued eastward into central Wisconsin and farther east as the Spirit Lake tectonic zone (SLtz). To test the age of Paleoproterozoic crust south of this structure, several subsurface samples of Precambrian basement from the north-central United States have been analyzed or re-examined using modern techniques of U–Pb, Sm–Nd, and $^{40}Ar/^{39}Ar$ geochronology. The results fill in a major data gap for the region and show that all U–Pb crystallization ages for samples south of the SLtz are geon 17 (1700–1800 Ma). Bedrock core samples from eastern Nebraska are ca. 1760–1800 Ma, and two samples from SE South Dakota, immediately south of the SLtz, yield ages of 1762 ± 28 Ma (Vermillion) and 1733 ± 2 Ma (Elk Point). Xenoliths from impact breccia in the Manson structure in north-central Iowa yield a similar age of ca. 1705 ± 30 Ma and metagabbro from SE Minnesota yields an age of 1760 ± 9 Ma. Farther to the northeast, zircons from Paleoproterozoic gneiss in the basement of Manitoulin Island, only a few km south of the Superior craton in Ontario, also yield a geon 17 age (1714 ± 10 Ma).

Sm–Nd model ages (T_{DM}) for samples immediately south of the SLtz fall in the range 1.9–2.2 Ga, indicating limited involvement of Archean crust. In contrast, Sm–Nd T_{DM} ages for samples north of the SLtz typically range from 2.5 to 3.0 Ga, for both Paleoproterozoic plutons and Archean gneisses. Ion microprobe analyses of zircons from the Elk Point and Manson samples also show the presence of geon 16 overgrowths, indicating a strong regional thermal overprint during geon 16 accretion. This is supported by mid-geon 16 hornblende $^{40}Ar/^{39}Ar$ ages for samples from SE South Dakota and SE Minnesota. Although no U–Pb ages are available for juvenile basement beneath the ca. 1760 Ma granite–rhyolite suite of southern Wisconsin, south of the SLtz, Sm–Nd model ages are typically ca. 1.9–2.0 Ga, consistent with basement to the rhyolites being geon 17 in age.

Collectively, the data require that most, if not all, of the Paleoproterozoic crust immediately south of the SLtz formed during geon 17 and probably represents eastward continuation, from Colorado, through Nebraska, of the Yavapai crustal province in the SW United States. Penokean (geon 18) crustal rocks are limited mainly to northern and central Wisconsin, east-central Minnesota, and northern Michigan. These results also show that medium grade (>500 °C) tectonothermal effects of the subsequent geon 16 (≈Mazatzal) orogeny to the south continue into the north-central United States. Both terranes probably also continue eastward into Ontario, Canada and farther east into protolith of the Grenville Province.

---

* Corresponding author. Tel.: +1 785 864 3676.
  E-mail address: rvschmus@ku.edu (W.R. Van Schmus).

1. Introduction

Over the past three decades substantial advances have been made in understanding the regional geology of mostly buried Precambrian crust in the Midcontinent region of the United States (cf. Sims and Peterman, 1986; Bickford et al., 1986; Van Schmus et al., 1993a,b, 1996; Rohs and Van Schmus, 2006). One of the remaining puzzles regarding the northern Midcontinent region has been defining eastward continuation of geon 17 (≈Yavapai) and geon 16 (≈Mazatzal) terranes of the transcontinental Proterozoic provinces (cf. Van Schmus et al., 1993a,b; CD-ROM Working Group, 2002) in such a way that it agrees with west–southwest continuation of the geon 18 Penokean orogen of the Great Lakes area (cf. Sims et al., 1989) and southward continuation of the coeval Trans-Hudson orogen (cf. Klasner and King, 1986, 1990). In particular, the few dated subsurface samples in Nebraska, Iowa, South Dakota, southeastern Minnesota, and southern Wisconsin have provided very limited information with which to constrain regional correlations of the Paleoproterozoic crust. Recently, however, several new sources of data can provide significant insights into this problem, with the consequence that the geology of the Precambrian basement in the north-central United States is undergoing major re-interpretation (see other papers in this volume).

We present in this paper new geochronologic data from basement core samples in southeastern Minnesota, northern Iowa, southeastern South Dakota, and northern Ontario. In addition, improvements in geochronological techniques over the past two decades allow us to study other samples that previously yielded too few accessory minerals for reliable analysis, to re-examine samples from previous studies which yielded imprecise results, or to re-interpret previous results in the light of new geophysical data. Collectively, our results indicate that most of the Paleoproterozoic crust south of the Archean craton (Superior Province) in Iowa and Minnesota is younger than 1800 Ma and therefore represents a general eastward continuation of geon 17 (≈Yavapai) and geon 16 (≈Mazatzal) terranes of the SW United States rather than westward continuation of the Penokean orogen as had commonly been shown on maps up to now (cf. Sims, 1990; Sims et al., 1993; Van Schmus et al., 1993a,b, 1996; CD-ROM Working Group, 2002). We also demonstrate that medium-grade thermotectonic events of geon 16 (≈Mazatzal or eastern correlative) orogenic events affected most of the region south of the Archean craton in the upper Midwest.

In order to facilitate discussion of broad correlations to the west in this paper, we will use the terms Yavapai and Mazatzal (cf. CD-ROM Working Group, 2002) to encompass crust formed and rapidly accreted to southern Laurentia between 1.80 and 1.70 Ga (geon 17; ≈Yavapai) and 1.70 and 1.60 Ga (geon 16; ≈Mazatzal), respectively. These timespans are somewhat broader age limits than commonly used for the Yavapai and Mazatzal orogens in Arizona–Colorado–New Mexico. We recognize that this is a major simplification that likely masks details of a rich and complex geologic history in the SW United States during the late Paleoproterozoic (cf. CD-ROM Working Group, 2002; Karlstrom et al., 2005). Given the limited crustal exposure and geochronologic control in the Midcontinent region, however, a more simplified broad-brush approach seems justified when attempting to correlate our results to those in better exposed and better-understood terranes to the west and east.

2. Regional geological relationships

2.1. Regional setting and study area

Fig. 1 shows a modified interpretation of the Precambrian basement geology in the north-central United States. Key modifications from prior renditions of this basement geology (e.g. Van Schmus et al., 1993a,b) include: (a) reduction in the southward extent of preserved Penokean-interval crust (1890–1830 Ma) and (b) eastward extension of geon 17 and geon 16 crust from Wyoming, Colorado, and New Mexico. A key structural element, which shows clearly on geophysical maps of the Midcontinent region, is a sharp transition that is now referred to as the Spirit Lake tectonic zone (SLtz; NICE Working Group, 2007); the SLtz cuts across NW Iowa and SE Minnesota and continues eastward into Wisconsin. In Iowa and Minnesota, crust north of the SLtz is comprised of Archean granite–gneiss complexes (Sims et al., 1993; Southwick, 1994; Windom et al., 1993); basement south of the SLtz is shown in this paper primarily to consist of geon 17 rocks. In Wisconsin the Marshfield terrane lies immediately north of the SLtz; it is mainly comprised of Archean continental crust that is intruded by several Penokean plutons (Van Schmus and Anderson, 1977; Van Schmus, 1980; Van Wyck, 1995).

The SLtz continues southwestward into SE South Dakota. Magnetic data (Klasner and King, 1986; Finn and Sims, 2005) and geochronological data (this paper) indicate that it turns northwestward, but it is still bounded on the north by Archean crust of the Superior Province (Klasner and King, 1986) and on the south by geon 17 crust. At some point the SW margin of the Superior Province becomes bounded by geon 18 rocks of the
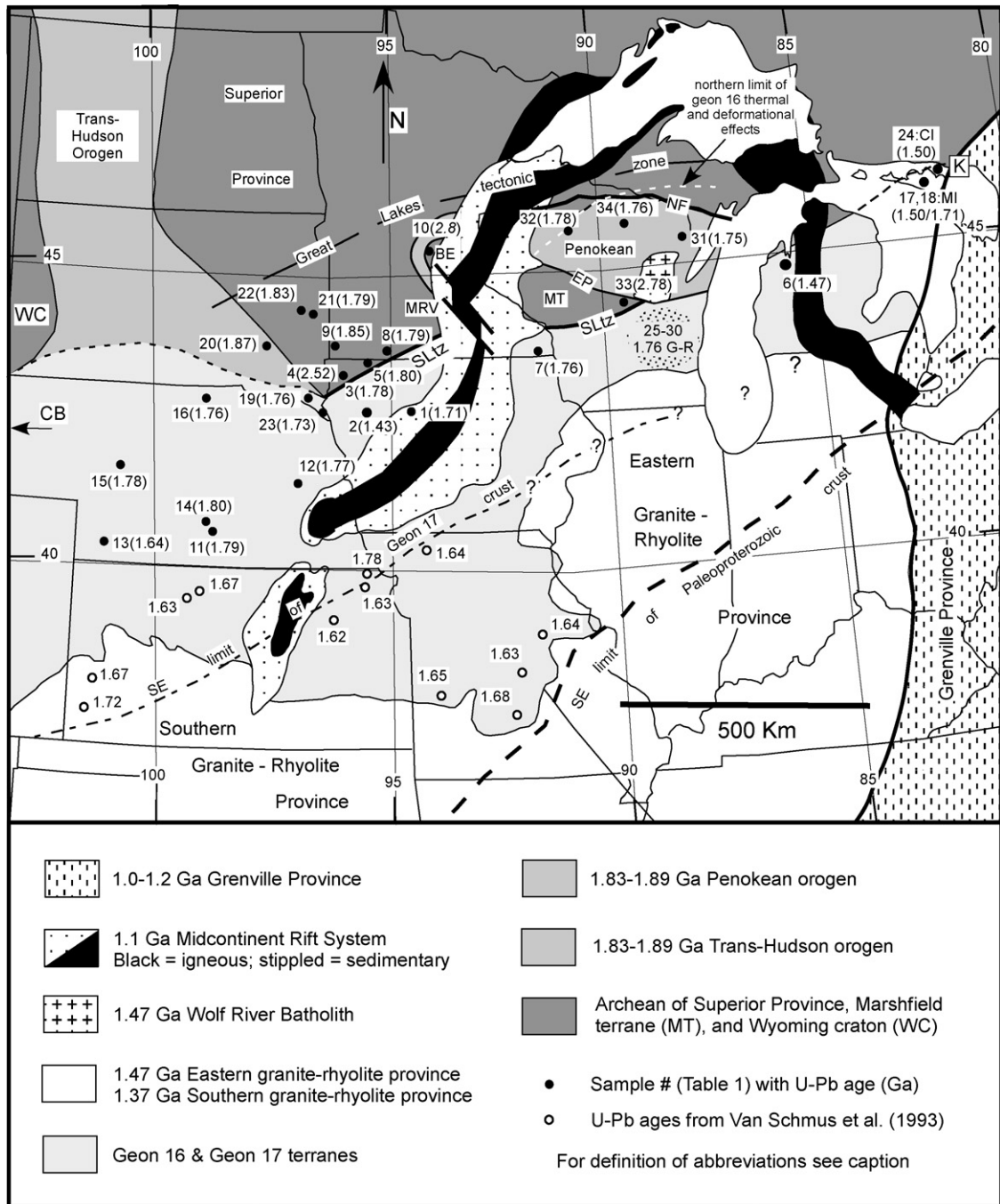
Fig. 1. Map of the northern Midcontinent region of the United States showing locations of samples and U–Pb ages discussed in this paper (sample numbers keyed to Table 1). Major province boundaries modified after Van Schmus et al. (1996) and NICE Working Group (2007). Dashed white line in northern Wisconsin–upper Michigan is northern limit of 1630 Ma resetting of Ar–Ar ages in Proterozoic quartzites (Holm et al., 1998b). Abbreviations: BE = Becker Embayment, CB = Cheyenne Belt, CI = Croker Island complex, EP = Eau Pleine shear zone, G–R = granite–rhyolite province, K = Killarney magmatic complex, MI = Manitoulin Island, MRV = Minnesota River Valley terrane prominitory, MT = Marshfield terrane, NF = Niagara Fault, SLtz = Sprit Lake tectonic zone, WC = Wyoming craton.

Trans-Hudson orogen (Klasner and King, 1986, 1990); the westward extension of the SLtz, if any, should be bounded on the north by geon 18 rocks. In south-central and southwestern South Dakota, however, the transition from geon 18 crust of the southern Trans-Hudson orogen to geon 17 crust of northern Nebraska is poorly constrained, with only one well-dated geon 17 basement sample in north-central Nebraska (NBKP-01: Van Schmus et al., 1993a; this paper).

In southern Wyoming and northern Utah the Archean–Paleoproterozoic transition is represented by the Cheyenne Belt (Karlstrom and Houston, 1984; Karlstrom and Humphreys, 1998; Karlstrom et al., 2005), which juxtaposes geon 17 rocks of the NE Mojave Province and northern Yavapai Province against Archean crust of the Wyoming craton to the north. These relationships will be discussed further toward the end of this paper.

There are several drill holes to basement along and on either side of the SLtz in South Dakota, Iowa, Minnesota, and Wisconsin that provide key age control (Table 1). New and re-evaluated ages for these samples provide key tests for our proposed chronologic similarity between the Cheyenne Belt and the Spirit Lake tectonic zone (geon 17 rocks juxtaposed with Archean cratonic rocks). These data also indicate, however, significant differences in their tectonic histories, as discussed below.

2.2. Prior geochronologic results

2.2.1. Basement crystallization ages

U–Pb zircon crystallization ages for juvenile crust exposed in central and northern Wisconsin definitively bracket the Penokean orogeny between 1880 and 1830 Ma (Van Schmus, 1976, 1980; Sims et al., 1989). However, a paucity of samples from Midcontinent basement to the south and west has left the age of that crust largely unconstrained. For example, the Precambrian basement of Iowa has commonly been portrayed as Penokean crust which was bounded by Archean crust to the north, similar to the geological relationship in northern Wisconsin along the Niagara Fault zone (a Paleoproterozoic suture), and Van Schmus et al. (1993b) argued that the Niagara Fault continued southwestward to the Spirit Lake trend in NW Iowa (contrary to our interpretation in this paper). In contrast, U–Pb zircon ages from basement drill hole samples in Nebraska are dominantly 1800 Ma or younger and probably represent eastward extension of geon 17 (≈Yavapai) basement of central and northern Colorado (Van Schmus et al., 1987, 1993a).

Previously published Paleoproterozoic zircon ages and Sm–Nd data from Nebraska, Kansas, and Missouri (Table 1; Figs. 1 and 2) show that geon 17 and geon 16 crust underlies most of the central Midcontinent region. Although data are sparsely distributed, one geon 17 drill hole in SE Kansas and another in NE Kansas (KSST-01 at 1716 ± 29 Ma and KSNM-21 at 1780 ± 20 Ma, respectively; Van Schmus et al., 1993a) suggest that the southern limit of geon 17 crust trends diagonally, SW–NE, across the state. This boundary (Figs. 1 and 2) is more or less in-line with the Jemez lineament in the southwest, which delineates a better controlled southern limit of Yavapai crust in Arizona and New Mexico (CD-ROM Working Group, 2002; Karlstrom et al., 2005). There are, however, no U–Pb crystallization ages for geon 17 primary crust in southern Iowa or southern Wisconsin that allow precise projection of this boundary eastward.

Sm–Nd crustal formation ages (T_{DM}) for Paleoproterozoic basement in the western Midcontinent region typically range between 1.8 and 2.0 Ga, and ca. 1450 Ma plutons intruded into this basement also commonly yield similar values (Van Schmus et al., 1993a, 1996). Such model ages do not occur south and east of a line trending approximately from southern Michigan–southern Ontario to West Texas and have been used by Van Schmus et al. (1993a, 1996) and Rohs and Van Schmus (2006) to define the S–SE limits of Paleoproterozoic crust in the Midcontinent (Fig. 1).

2.2.2. Metamorphism and deformation

Metamorphism along the southern margin of the Archean Superior Province has been historically attributed to Penokean-interval orogenesis. Indeed, a narrow window of amphibolite-facies rocks north of the Niagara Fault zone in the southern Lake Superior region does record 1.83–1.80 Ga monazite U–Th–Pb crystallization ages (Schneider et al., 2004; Holm et al., 2007). Peak metamorphic conditions with attendant magmatism at ca. 1.83 Ga probably represent the culmination of Penokean arc accretion. The dominant metamorphic and igneous imprint on basement rocks in the Archean–Penokean boundary area, however, is a regional tectonothermal event dated at ca. 1.76 Ga (Holm et al., 1998a; Schneider et al., 2004) and includes the 1775 Ma east-central Minnesota batholith (Holm et al., 2005). This is a style and age of deformation similar to that in the southwestern U.S. (CD-ROM Working Group, 2002), where Yavapai convergence resulted in widespread thermal overprinting and significant magmatism during geon 17. In the Lake Huron region of Ontario, geon 17 magmatism and metamorphism are

Table 1
Summary of sample locations, zircon ages, and Sm/Nd data from the northern Midcontinent region

Sample number	Sample identity	Rock type	County	Section	Township	Range	W Long	N Lat	Zircon age (Ma)	Sm/Nd T_{DM}	References	
											Zirc	Nd
1. IA-M8	Manson drill hole M8	Gneiss, granite	Pocahontas	16	90N	31W	94.51	42.60	1705 ± 30	*	00	
2. IACK-01	Kans. Univ. #1 Peterson	Granite	Cherokee	34	90N	41W	95.67	42.57	1433 ± 06	1.84	V4	V4
3. IALY-07	N J Zinc, Matlock C5.914	Keratophyre	Lyon	28	98N	44W	96.05	43.28	1782 ± 04	2.70	W1	W1
4. IALY-09	N J Zinc, Matlock C10.706	Monzodiorite	Lyon	25	98N	44W	95.98	43.27	2523 ± 05	2.91	W1	W1
5. IAOS-01	Iowa Geol Surv, D-13 Test	Granite	Osceola	17	100N	39W	95.48	43.45	1804 ± 19	2.30	V3	00
6. MIGT-01	Shell State Blair #24	Granite	Grand Trav.	24	26N	11W	85.58	44.63	1472 ± 02	1.90	H1	00
7. MNFI-01	MNGS Drill hole BO-1	Metagabbro	Fillmore	22	101N	8W	91.78	43.54	1760 ± 09	1.73	00	00
8. MNJK-01	MNGS, DH SQ-5	Granite	Jackson	11	102N	36W	95.14	43.65	1792 ± 31	2.20	S1	00
9. MNPS-01	Outcrop, MNGS SX-60PEB	Metarhyolite	Pipestone	36	106N	47W	96.45	43.94	*ca. 1850*	2.14	W2	00
10. MNSH-01	MNGS DH T101A	Gd. gneiss	Shelburne	19	34N	28W	93.87	45.42	*ca. 2800*	3.18	est.	00
11. NBBF-01	Ohio Oil, #1 Pettett	Tonalitic gneiss	Buffalo	20	9N	18W	99.38	40.73	1787 ± 09	1.90	V3	V5
12. NBBU-01	Magness Petrol, #1 Orfan	Dioritic gneiss	Butler	5	13N	2E	97.23	41.13	1771 ± 09	1.87	V5†	V5
13. NBCS-02	Ohio Oil, #1 Bremer	Granodiorite	Chase	5	7N	39W	101.77	40.60	1639 ± 12		V5†	
14. NBDA-02	Ohio Oil, #1 Dunse	Granodiorite	Dawson	1	10N	19W	99.43	40.87	1802 ± 04		V3	
15. NBHK-01	Murfin Drilling, 1-33 Haney	Tonalitic gneiss	Hooker	33	21N	33W	101.14	41.75	1781 ± 08		V5†	
16. NBKP-01	Gerber Energy, B-1 Baker	Brecciated granite	Keya Paha	8	34N	19W	99.58	42.84	1760 ± 19	2.03	V5†	V5
17. ONMI-01a	Union Carbide #1, 1189′	Granite	n.a.		n.a.		82.76	45.86	1500 ± 20	2.09	V1	00
17. ONMI-01b	Union Carbide #1, 1308′	Aplite	n.a.		n.a.		82.76	45.86	1500 ± 20	1.98		00
18. ONMI-02a	Union Carbide #2, 2346′	Granitic gneiss	n.a.		n.a.		82.76	45.86	1714 ± 10	2.31	00	00
18. ONMI-02b	Union Carbide #2, 2391′	Migmatite	n.a.		n.a.		82.76	45.86	1714 ± 10	2.19		00
19. SDCL-01	SDGS, "Vermillion"	Granite	Clay	14	92N	52W	96.95	42.78	1762 ± 28	2.08	V5†	V5
20. SDDA-01	SDGS #1 Everett Wilson	Granodiorite	Davison	25	103N	61W	98.10	43.69	1871 ± 16	2.55	00	00
21. SDMO-01	Kerr-McGee, Mineral Test	Granophyric gr.	Moody	1	106N	49W	96.65	44.01	1790 ± 13	2.57	V5†	V5
22. SDMO-02	Kerr-McGee, Mineral Test	Metarhyolite	Moody	30	107N	49W	96.74	44.04	1828 ± 08	2.59	V5†	V5
23. SDUN-01	SDGS, "Elk Point"	Metagabbro	Union	13	90N	50W	96.70	42.62	1733 ± 02	2.17	00	00
24. VS62-13	N. Benjamin I., Ontario	Granite	n.a.		n.a.		82.26	46.09	*ca. 1500*	2.02	V1	00
25. VS70-01	Outcrop, Berlin, WI	Metarhyolite	Waushara	3	17N	13E	88.93	43.97	*ca. 1760*	1.94	V6	00
26. VS70-06	Outcrop, Utley, WI	Metarhyolite	Green Lake	36	15N	13E	88.90	43.73	*ca. 1760*	1.91	V6	00
27. VS70-07	Outcrop, Marquette, WI	Metarhyolite	Green Lake	34	15N	11E	89.17	43.74	*ca. 1760*	1.94	V6	00
28. VS70-82	Outcrop, Endeavor, WI	Metarhyolite	Marquette	5	14N	9E	89.45	43.72	*ca. 1760*	1.91	V6	00
29. VS70-83	Outcrop, Observatory Hill, WI	Metarhyolite	Marquette	8	14N	10E	89.34	43.70	1759 ± 02	1.92	H2	00
30. VS73-01B	Outcrop, Utley, WI	Metarhyolite	Green Lake	36	15N	13E	88.90	43.73	*ca. 1760*	1.94	V6	00
31. VS73-08	Outcrop, Amberg, WI	Granite	Marinette	3	35N	20E	87.98	45.53	1754 ± 11	2.01	H2	00
32. VS73-37	Outcrop, Radisson, WI	Granite	Saywer	22	38N	7W	91.22	45.76	1776 ± 08	2.41	H2	00
33. VS76-37A	Outcrop, Linwood Twp., WI	Migmatite	Portage	15	23N	7E	89.65	44.47	*ca. 2800*	3.02	V2	D1
34. "23"	Outcrop, S. of Monico, WI	Granite	Oneida	6	35N	11E	89.16	45.54	ca. 1760	2.09	V6	B1

Notes: Sample numbers mostly from Van Schmus field notes or University of Kansas *Project Upper Crust* sample numbers (State–County–Number). Sec–Twp–Rge = section–township–range; W Long = west longitude; N Lat = north latitude; ages $\pm 2\sigma$; T_{DM} ages in Ga; *: sample too altered for whole-rock analysis. n.a. = not applicable. Italicized age estimates based on regional geology (est.) or general zircon ages as referenced. Numbers following ONMI samples refer to dept (in feet) below the surface for core pieces analyzed. References: B1, Barovich et al. (1989); D1, Dewane and Van Schmus (2007); H1, Hoppe et al. (1983); H2, Holm et al. (2005); S1, Southwick (1994); V1-Van Schmus et al. (1975b); V2, Van Schmus and Anderson (1977); V3, Van Schmus et al. (1987); V4, Van Schmus et al. (1989); V5, Van Schmus et al. (1993a). †: detailed U–Pb or Sm–Nd data not published; U–Pb ages quoted here may differ slightly due to additional analyses or to refinement in calculations; V6, Van Schmus (1980); W1, Windom et al. (1993); W2, Wallin and Van Schmus (1988); 00, this study.
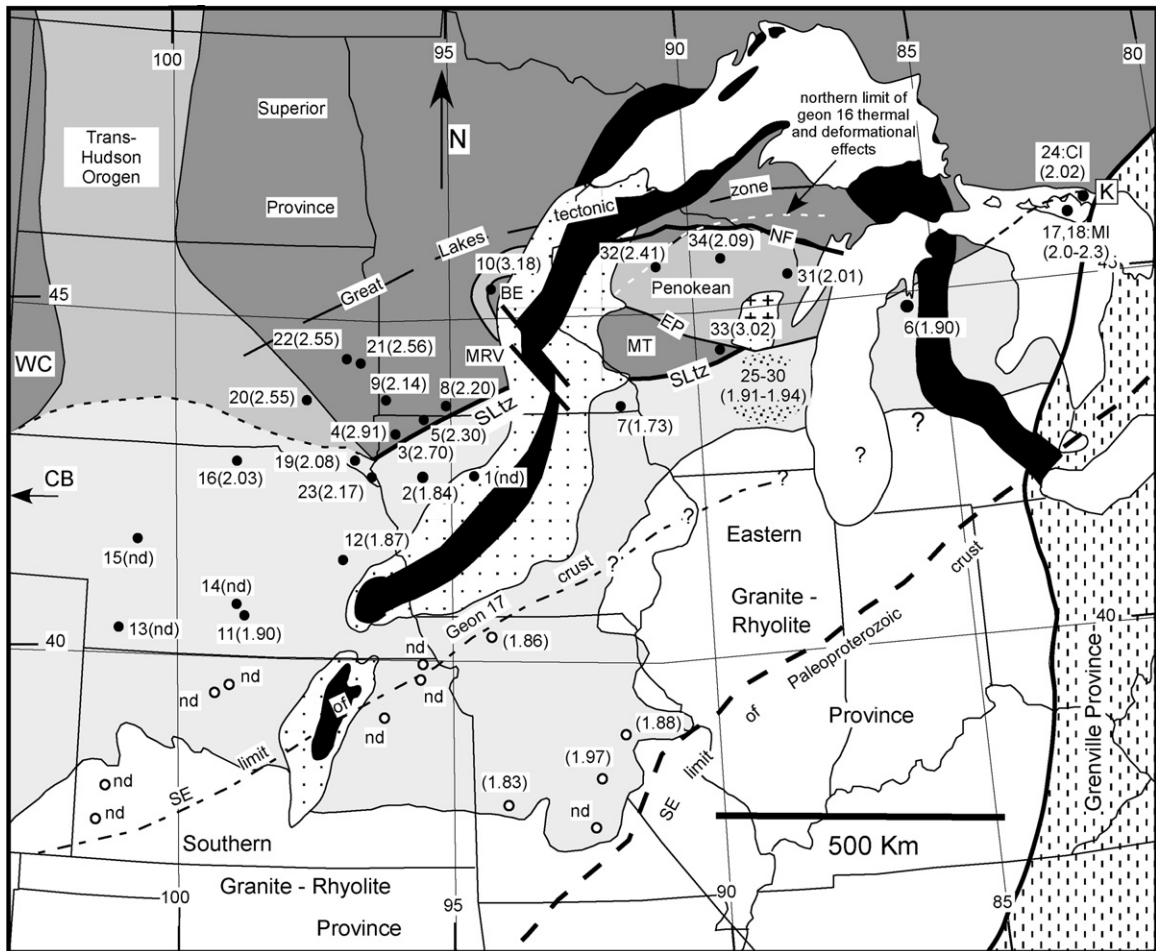
Fig. 2. Map of the northern Midcontinent region of the United States showing locations of samples and Sm–Nd T_{DM} ages discussed in this paper (sample numbers keyed to Table 1); n.d. = not determined. See Fig. 1 for legend and other information.

the dominant tectonothermal event south of the Archean shield as well (Piercey et al., 2007).

Thermochronometric studies from basement rocks of the north-central Midcontinent have revealed detailed characteristics of its Proterozoic lower temperature history (Holm and Lux, 1996; Schneider et al., 1996; Romano et al., 2000; Holm et al., 2007). Penokean-interval $^{40}Ar/^{39}Ar$ biotite cooling ages are only preserved in low-grade arc rocks in east-central Minnesota; a few hornblende ages also record Penokean cooling in metasedimentary rocks of the orogen. Elsewhere throughout the Lake Superior and Lake Huron region, hornblende and mica $^{40}Ar/^{39}Ar$ ages are predominantly 1.76–1.75 Ga or somewhat younger (see summary Fig. 4 of Schneider et al., 2004), reflecting rapid, widespread cooling and orogenic collapse following the afore-mentioned geon 17 amphibolite-facies metamorphism and magmatism.

Across much of the Wisconsin Precambrian bedrock, low-temperature (300 °C) reheating coeval with deformation was responsible for resetting whole-rock Rb–Sr ages (Van Schmus et al., 1975a; Van Schmus, 1978; Medaris et al., 2003) and $^{40}Ar/^{39}Ar$ mica cooling ages (Holm et al., 1998b; Romano et al., 2000). This resetting is inferred to have been broadly related to geon 16 (≈Mazatzal) accretion to the south in the central Midcontinent region. Deformed Baraboo Interval quartzites (1760 Ma > t > 1630 Ma) accurately delineate the region of geon 16 (≈Mazatzal) deformation. The northern limit of this deformation and moderate temperature (300–500 °C) reheating is approximately located along the Niagara Fault zone in northern Wisconsin and upper Michigan (Fig. 1). In Minnesota the deformational front must trend south of the Minnesota River Valley promontory of Archean basement, since those rocks are not isotopically reset and are overlain by flat-lying Baraboo

Interval quartzites (Sioux quartzite; Holm et al., 1998b); Fig. 1 shows the NW limit of this geon 16 deformational and metamorphic front. Geon 16 heating is recorded only locally in the Lake Huron region of the orogen (Piercey et al., 2007).

Intrusion of the 1.47 Ga Wolf River batholith and other related geon 14 A-type plutons across the northern Midcontinent only had a limited thermal effect on the surrounding country rock, in part reflecting their rapid emplacement at shallow crustal levels. Hydrothermal alteration along the Paleoproterozoic basement/cover contact did occur, however, at considerable distances from the batholith (Medaris et al., 2003). In contrast, geon 14 magmatism in the southwestern United States was accompanied by pervasive thermal effects, causing a major regional resetting of $^{40}Ar/^{39}Ar$ ages throughout the Yavapai–Mazatzal basement (Shaw et al., 2005). Geon 14 magmatism was ubiquitous throughout the central Midcontinent (cf. Van Schmus et al., 1993a), but few reliable data exist relevant to the intensity of reheating the older Paleoproterozoic crust in the region during this event.

3. New geochronologic data and re-interpretation of prior results

3.1. U–Pb analyses

TIMS U–Pb data (Table 2) were obtained by Van Schmus and colleagues at the Isotope Geochemistry Laboratory (IGL), University of Kansas over an interval of about 25 years. The older data (1980s) were obtained using relatively large (few mg), multi-grain fractions; zircons were dissolved and Pb and U were separated using procedures modified after Krogh (1973, 1982; see Bowring et al., 1984 for further details). Some ages and accompanying data were published by Van Schmus et al. (1987), whereas only ages were published for additional samples by Van Schmus et al. (1993a). Table 2 includes data for individual zircon fractions from all samples for which the detailed data were not previously published. In those cases where our files no longer include actual measurement errors, uncertainties of ±1% were assigned for U/Pb ratios, $^{207}Pb*/^{206}Pb*$ ratios were assigned an error of ±0.2%, and correlation coefficients (ρ) were assigned a corresponding value of 0.980. Over the past 20 years experience has shown that these values are consistent with values (0.5–1.0%, 0.05–0.2%, and 0.980–0.990%, respectively) typically obtained using PBDAT (Ludwig, 1988) for data reduction.

More recent (2005–2006) data were obtained from single-grain analyses using procedures modified after Krogh (1973) and Parrish (1987). In these single-crystal analyses the entire dissolved sample was loaded on a Re filament using phosphoric acid and silica gel without prior ion-exchange column purification (Bruguier et al., 1994). The U–Pb isotopic analyses were done in single-collector mode using an ion-counting Daly system on a VG Sector mass spectrometer and measured as Pb^+ and UO_2^+.

Lead compositions were corrected for mass discrimination (typically 0.10–0.12% per amu) as determined by analysis of NBS SRM-982 (equal-atom) Pb and monitored by analysis of NBS SRM-983 (radiogenic) Pb; uranium fractionation was monitored by analyses of NBS SRM U-500. Radiogenic ^{208}Pb, ^{207}Pb, and ^{206}Pb was obtained by correcting for modern blank Pb and for non-radiogenic original Pb corresponding to Stacey and Kramers (1975) model Pb for the approximate age of the sample. Uncertainties in radiogenic Pb ratios are typically less than ±0.1% at the 2σ level unless the samples had a low $^{206}Pb/^{204}Pb$ ratio, in which case errors in the common Pb correction could cause greater uncertainties. Decay constants used were 0.155125×10^{-9} year^{-1} for ^{238}U and 0.98485×10^{-9} year^{-1} for ^{235}U (Steiger and Jäger, 1977). Blanks were about 2 ng total Pb in 1982 and about 2–4 pg total Pb in 2005; in all cases they do not contribute significantly to uncertainties in the ages of samples. Data reduction followed PBDAT of Ludwig (1988).

Zircon data were regressed for this paper using the Isoplot/Ex program (Ludwig, 2001). Model 1 regressions were accepted if probabilities of fit were better than 20%. Model 2 regressions were used if probabilities of fit were less than 20%; in the latter case uncertainties in concordia intercept ages were recalculated to the 2σ level using the appropriate Student's t-multiplier for the number of analyses regressed. Results are summarized in Table 2 and presented in Figs. 1 and 3. For older analyses (Van Schmus et al., 1987, 1993a) ages may differ slightly from previously published values due to use of updated regression methods.

For three drill core samples, SDUN-01 (South Dakota), IA-M8 (Manson structure, Iowa) and ONMI-02 (Manitoulin Island, Ontario), single-spot SIMS U–Pb zircon ages were measured by two of us (Schneider and Dodson) using the Cameca ims1270 ion microprobe at the University of California, Los Angeles. Rock cores were processed for zircon through standard mineral separation techniques, including heavy liquid and magnetic separation. Prior to isotopic analysis, the zircon grains were mounted with an age standard in an epoxy probe mount and imaged with BSE/SEM techniques. Most grains showed some sector zoning that is probably a

Table 2

New and previously unreported data for individual zircon fractions from northern Midcontinent basement samples

Sample / Fraction	Size (mg)	U (ppm)	Pb (ppm)	$\frac{206\text{Pb}}{204\text{Pb}}$ (obs.)	Isoplot data $\frac{207\text{Pb*}}{235\text{U}}$	± 2σ (%)	$\frac{206\text{Pb*}}{238\text{U}}$	± 2σ (%)	Correlation coefficient (ρ)	$\frac{207\text{Pb*}}{206\text{Pb*}}$	± 2σ (%)	Calculated Ages $\frac{206\text{Pb*}}{238\text{U}}$ Age (Ma)	± 2σ (Ma)	$\frac{207\text{Pb*}}{235\text{U}}$ Age (Ma)	± 2σ (Ma)	$\frac{207\text{Pb*}}{206\text{Pb*}}$ Age (Ma)	± 2σ (%)
IAOS-01: Osceola Co.; granite																	
NM(0)	2.100	226	65	904	3.7230	3.09	0.24611	3.09	0.999	0.10972	0.11	1418	44	1576	49	1795	2
M(0)	3.300	253	67	1642	3.4951	0.52	0.23287	0.52	0.992	0.10885	0.07	1350	7	1526	8	1780	2
M(1)	2.000	322	75	1250	3.0330	0.56	0.20198	0.55	0.990	0.10891	0.08	1186	7	1416	8	1781	2
M(2)	2.800	412	88	744	2.6443	0.60	0.17745	0.59	0.986	0.10807	0.10	1053	6	1313	8	1767	2
Regression: U.I. = 1804 ± 19 Ma, L.I. = 84 ± 65 Ma; *P* < 0.01 (Model 2, 2σ)																	
MNFI-01: Fillmore Co. (MNGS BO-1; 1335′ depth); metagabbro																	
HP-a	0.003	506	163	4486	4.6252	1.11	0.31104	1.10	0.992	0.10785	0.14	1746	19	1754	19	1763	3
HP-b	0.003	404	128	5172	4.6373	0.51	0.31278	0.50	0.974	0.10753	0.12	1754	9	1756	9	1758	2
HP-c	0.002	81	26	550	3.9013	1.20	0.26181	0.99	0.861	0.10807	0.61	1499	15	1614	19	1767	11
Regression: U.I. = 1760 ± 9 Ma, L.I. = 0 ± 10 Ma (forced); *P* < 0.01 (Model 1; 2σ)																	
NBBF-01: Buffalo Co.; tonalitic gneiss																	
M(0)	4.000	362	100	1658	3.9999	0.64	0.26712	0.63	0.987	0.10860	0.10	1526	10	1634	10	1776	2
M(1)	3.300	478	115	1057	3.3820	0.51	0.22677	0.48	0.963	0.10817	0.14	1318	6	1500	8	1769	3
M(2)	0.500	405	83	636	2.9740	1.28	0.20093	1.27	0.988	0.10735	0.20	1180	15	1401	18	1755	4
Regression: U.I. = 1787 ± 9 Ma, L.I. = 97 ± 41 Ma; *P* = 0.02 (Model 2, 2σ)																	
NBBU-01: Butler Co.; dioritic gneiss																	
lg pk	1.11	114	31	11628	4.7610	1.00	0.31770	1.00	0.980	0.10867	0.20	1779	18	1778	18	1777	4
sm pk	0.307	142	38	2717	4.5780	1.00	0.30800	1.00	0.980	0.10779	0.20	1731	17	1745	17	1762	4
sm brn	0.324	410	109	7092	4.6020	1.00	0.30810	1.00	0.980	0.10832	0.20	1731	17	1750	18	1771	4
lg brn	0.454	394	44	3876	1.9080	1.00	0.12790	1.00	0.980	0.10820	0.20	776	8	1084	11	1770	4
Regression: U.I. = 1771 ± 9 Ma, L.I. = 3 ± 51 Ma; *P* < 0.01 (Model 2, 2σ)																	
NBCS-02: Chase Co.; granodiorite																	
NM(0)	6.40	201	47	2646	3.0440	1.00	0.21990	1.00	0.980	0.10037	0.20	1282	13	1419	14	1631	3
M(1)	7.80	294	60	2451	2.6310	1.00	0.18990	1.00	0.980	0.10051	0.20	1121	11	1309	13	1634	3
M(3)	8.06	397	65	1409	2.0420	1.00	0.14840	1.00	0.980	0.09981	0.20	892	9	1130	11	1621	3
Regression: U.I. = 1639 ± 12 Ma, L.I. = 32 ± 38 Ma; *P* = 0.03 (Model 2, 2σ)																	
NBDA-02: Dawson Co.; granodiorite																	
M(1)	1.9	470	119	1344	3.7480	1.00	0.24660	1.00	0.980	0.11025	0.20	1421	14	1582	16	1804	4
M(2)	1.9	467	112	953	3.4770	1.00	0.22880	1.00	0.980	0.11022	0.20	1328	13	1522	15	1803	4
M((3)	1.4	561	131	781	3.3460	1.00	0.22060	1.00	0.980	0.11001	0.20	1285	13	1492	15	1800	4
M(4)	1.2	683	116	526	2.3720	1.00	0.15610	1.00	0.980	0.11021	0.20	935	9	1234	12	1803	4
Regression: U.I. = 1802 ± 4 Ma, L.I. = −1 ± 12 Ma; *P* = 0.25 (Model 1, 2σ)																	
NBHK-01C: Hooker Co.; tonalitic gneiss																	
M(-1)AA	2.84	203	63	4762	4.5550	1.00	0.30360	1.00	0.980	0.10881	0.20	1709	17	1741	17	1780	4
M(-2)	2.43	161	48	2762	4.3240	1.00	0.28770	1.00	0.980	0.10900	0.20	1630	16	1698	17	1783	4
M(-1)	2.34	193	57	3610	4.2940	1.00	0.28580	1.00	0.980	0.10899	0.20	1620	16	1692	17	1782	4
M(0)	3.06	230	66	3636	4.1510	1.00	0.27690	1.00	0.980	0.10872	0.20	1576	16	1664	17	1778	4

Table 2 (*Continued*)

Sample	Fraction	Size	U	Pb	$\frac{206\text{Pb}}{204\text{Pb}}$	Isoplot data					$\frac{207\text{Pb*}}{206\text{Pb*}}$	±2σ	Calculated Ages					
						$\frac{207\text{Pb*}}{235\text{U}}$	±2σ	$\frac{206\text{Pb*}}{238\text{U}}$	±2σ	Correlation coefficient.			$\frac{206\text{Pb*}}{238\text{U}}$	±2σ	$\frac{207\text{Pb*}}{235\text{U}}$	±2σ	$\frac{207\text{Pb*}}{206\text{Pb*}}$	±2σ
		(mg)	(ppm)	(ppm)	(obs.)		(%)		(%)	(ρ)		(%)	Age	(Ma)	Age	(Ma)	Age	(%)
	Regression: U.I. = 1781 ± 8 Ma, L.I. = 10 ± 140 Ma; *P* = 0.12 (Model 2, 2σ)																	
NBKP-01: Keya Paha Co.; brecciated granite																		
	NM(4)	1.420	398	95	2326	3.2994	1.00	0.22293	1.00	0.980	0.10734	0.20	1297	13	1481	15	1755	4
	NM(2)	0.095	248	58	1721	3.1932	1.00	0.21353	1.00	0.980	0.10832	0.20	1248	12	1456	15	1772	4
	M(2)	0.109	449	62	824	1.7695	1.00	0.11790	1.00	0.980	0.10875	0.20	718	7	1034	10	1779	4
	M(6)	0.076	588	62	914	1.4104	1.00	0.09415	1.00	0.980	0.10853	0.20	580	6	893	9	1775	4
	Regression: U.I. = 1760 ± 19 Ma, L.I. = −19 ± 39 Ma, *P* < 0.01 (Model 2; 2σ)																	
SDCL-001: Vermillion, Clay County; granite																		
	NM(2)	0.087	377	75	1071	2.7638	1.00	0.17947	1.00	0.980	0.11159	0.20	1064	11	1346	13	1825	4
	NM(4)a	0.100	481	75	741	2.0609	1.00	0.13712	1.00	0.980	0.10894	0.20	828	8	1136	11	1782	4
	NM(4)b	0.094	388	63	680	2.1176	1.00	0.14221	1.00	0.980	0.10791	0.20	857	9	1154	12	1765	4
	M(4)a	0.119	728	81	283	1.2821	1.00	0.08532	1.00	0.980	0.10895	0.20	528	5	838	8	1782	4
	M(4)b	0.084	706	72	424	1.2555	1.00	0.08310	1.00	0.980	0.10952	0.20	515	5	826	8	1791	4
	Regression (analyses 2–5): U.I. = 1762 ± 28 Ma, L.I. = −19 ± 32 Ma, *P* < 0.01 (Model 2; 2σ)																	
SDDA-001: Davison County; granite																		
	M(0)AA	2.327	466	140	1575	4.2779	0.48	0.2717	0.47	0.980	0.11418	0.07	1550	7	1689	8	1867	1.3
	M(0)	0.139	387	66	944	2.4027	1.00	0.15065	1.00	0.980	0.11563	0.20	905	9	1243	12	1890	4
	M(2)	0.096	471	59	656	1.7100	1.00	0.10884	1.00	0.980	0.11392	0.20	666	7	1012	10	1863	4
	M(4)	0.078	540	80	90	1.4309	1.00	0.08964	1.00	0.980	0.11564	0.20	553	6	902	9	1890	4
	M(6)	0.089	687	45	358	0.8271	1.00	0.05303	1.00	0.980	0.11309	0.20	333	3	612	6	1850	4
	Regression: U.I. = 1871 ± 16 Ma, L.I. = −4 ± 24 Ma, *P* < 0.01 (Model 2; 2σ)																	
SDMO-01: Moody Co.; granophyric granite																		
	NM(0)AA	3.806	107	40	505	4.5602	0.57	0.30300	0.54	0.950	0.10880	0.18	1711	9	1742	10	1779	3
	NM(0)	1.230	160	54	189	3.5425	1.00	0.23588	1.00	0.980	0.10892	0.20	1365	14	1537	15	1781	4
	M(0)	1.340	178	56	197	3.3087	1.00	0.21915	1.00	0.980	0.10950	0.20	1277	13	1483	15	1791	4
	M(1)	1.830	218	62	190	2.8802	1.00	0.19291	1.00	0.980	0.10829	0.20	1137	11	1377	14	1771	4
	M(2)	2.630	237	61	181	2.5394	1.00	0.17119	1.00	0.980	0.10758	0.20	1019	10	1283	13	1759	4
	Regression: U.I. = 1790 ± 13 Ma, L.I. = 50 ± 38 Ma, *P* < 0.01 (Model 2; 2σ)																	
SDMO-002: Moody Co.; metarhyolite																		
	NM	2.818	127	48	340	4.3267	1.00	0.28145	1.00	0.980	0.11150	0.20	1599	16	1699	17	1824	4
	M(2)AA	4.338	106	42	675	4.9078	1.00	0.31957	1.00	0.980	0.11138	0.20	1788	18	1804	18	1822	4
	M(2)	4.700	127	52	255	4.3541	1.00	0.28242	1.00	0.980	0.11181	0.20	1604	16	1704	17	1829	4
	M(4)	3.888	131	59	175	4.3239	1.00	0.28068	1.00	0.980	0.11173	0.20	1595	16	1698	17	1828	4
	M(6)	3.498	134	65	135	4.2859	1.00	0.27666	1.00	0.980	0.11235	0.20	1575	16	1691	17	1838	4
	Regression: U.I. = 1828 ± 8 Ma, L.I. = 0 ± 0 Ma (forced); *P* < 0.01 (Model 1; 2σ)																	
SDUN-01: Elk Point, Union Co.; metagabbro																		
	NM(0)a	0.003	121	49	527	5.2034	0.73	0.35414	0.72	0.982	0.10656	0.14	1954	14	1853	14	1741	3
	NM(0)b	0.002	234	83	1313	4.8495	0.75	0.33039	0.72	0.954	0.10645	0.23	1840	13	1794	14	1740	4
	NM(0)c	0.001	242	81	1031	4.7898	1.01	0.32621	1.00	0.991	0.10649	0.14	1820	18	1783	18	1740	3
	NM(0)d	0.002	399	130	462	3.7880	0.63	0.26198	0.59	0.937	0.10487	0.22	1500	9	1590	10	1712	4
	Regression (analyses 2–4): U.I. = 1733 ± 2 Ma.; L.I. = 213 ± 33 Ma, *P* = 0.42 (Model 1, 2σ)																	

Notes: AA = air abraded (Krogh, 1982); M = magnetic; NM = non-magnetic; (*n*) = side tilt used on magnetic separator track during preparation of magnetic fractions; Letters a, b, c, d refer separate analyses from same magnetic split; HP = hand picked; lg = large; sm = small; brn = brown; pk = pink. Data regressed using Isoplot/Ex (Ludwig, 2001); uncertainties reported at the 2σ level (see text); U.I. = upper intercept on concordia; L.I. = lower intercept on concordia. Raw data reduced using PBDAT (various versions); where errors were not propagated during reduction, estimated values are given in italics (see text). *: Pb data corrected for analytical blank Pb and non-radiogenic Pb using Stacey and Kramers (1975) model Pb. All ages calculated using decay constants recommended by Steiger and Jäger (1977). See text for further details.
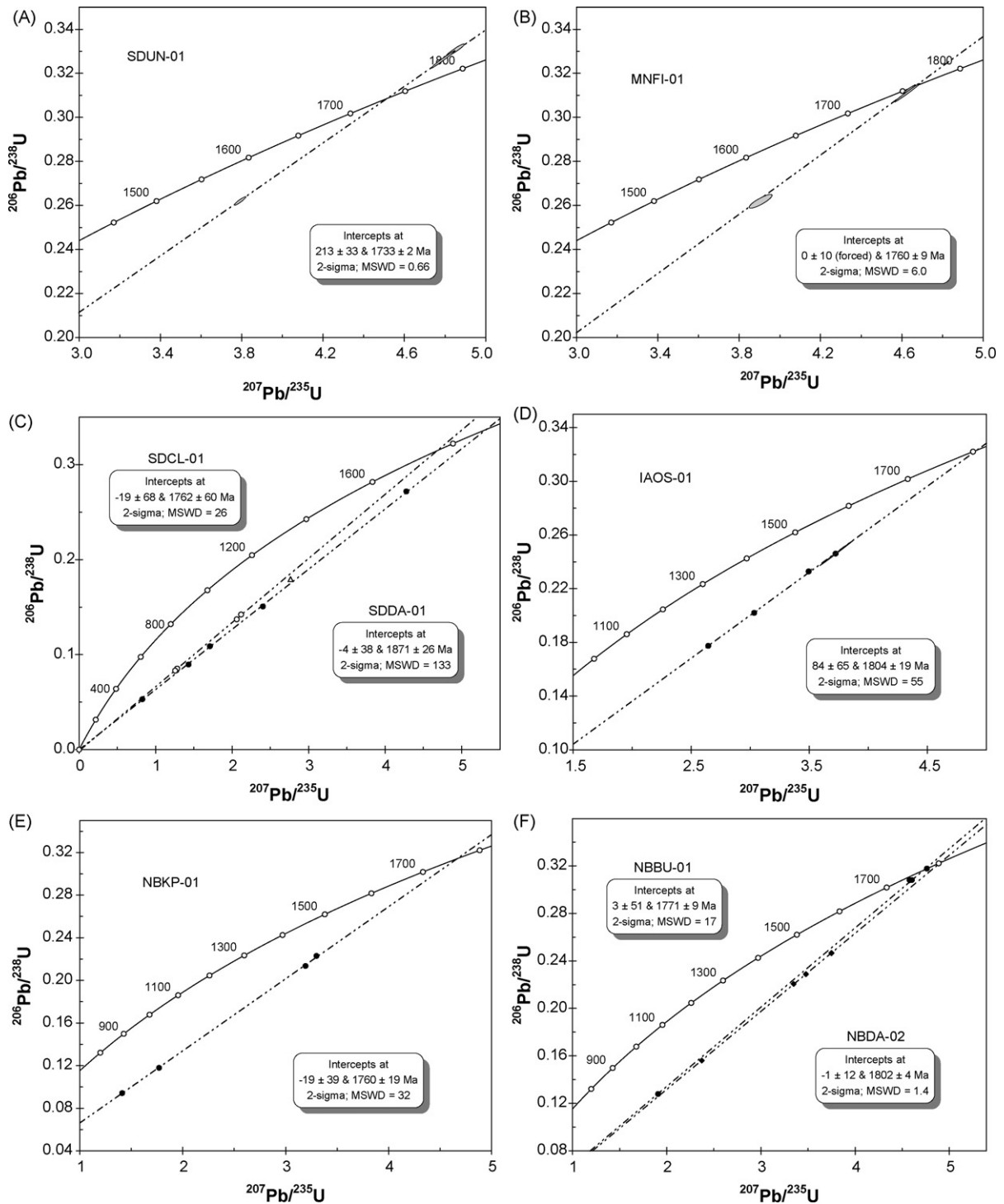
Fig. 3. Concordia plots of TIMS U–Pb data for selected samples discussed in this paper. (A) Single-crystal analyses for SDUN-01, metagabbro from Elk Point, Union County, South Dakota. (B) Single-crystal analyses for MNFI-01, metagabbro from MNGS drill hole BO-1 in Fillmore Co., Minnesota. (C) Previously unpublished multi-grain data for sample SDCL-01, a granite from Vermillion, Clay Co., South Dakota (open circles; open triangle omitted from regression) and SDDA-01, a granite from Davison Co., South Dakota (solid circles). (D) Previously unpublished multi-grain data for sample IAOS-01, a granite from Osceola Co., Iowa. (E) Previously unpublished multi-grain data for sample NBKP-01, a metagranite from Keya Paha County, Nebraska. (F) Previously unpublished multi-grain data for samples NBBU-01 (solid circles) and NBDA-02 (solid diamonds) in Nebraska. See text for further details and discussion.

primary igneous texture, with relatively thin, if any, overgrowths. Grains selected for analysis were intact grains with no embayments or other textural anomalies. Fifteen zircons each from SDUN-01 and IA-M8 were analyzed; 30 zircons were analyzed from ONMI-02. Most zircons were small (<80 μm), and were analyzed only once (single spot), so it is difficult to assess core-rim age relationships.

For isotopic analyses, the primary O^- ion beam was focused to a 15 μm × 20 μm spot. The standard operating conditions were a primary intensity of 3–4 nA, mass resolving power of ~4500, and a 50 eV energy window. Zircon U–Pb ages were determined relative to the zircon age standard AS3 (1099 ± 1 Ma; Paces and Miller, 1993). The precision of the method is not limited by counting statistics but by the reproducibility of the standard calibration curve, which is typically ±1–2% (Harrison et al., 1995). Uranium and thorium concentrations were estimated semiquantitatively by comparing peak intensities in the unknowns to those in standard AS3, which has a mean concentration of ~400 ppm Th and ~550 ppm U. Isotopic data, ages, and errors (±1σ) reported in Table 3 were obtained by data reduction and age calculations based on the methods of Harrison et al. (1995) and Catlos et al. (2002).

The data for each sample are variably discordant and show significant lateral scatter in $^{207}Pb/^{206}Pb$ ages. To further resolve the SIMS data, we systematically eliminated some of the dates from the regression procedure. The data that have been included in the upper intercept age calculations (Fig. 4) have small errors (<20 m.y.), are concordant or normally discordant, and have Th/U ratio >0.2. There is a clear relationship between the chemistry of zircon and the processes which operate during accessory mineral genesis, and a general association between zircon of "metamorphic" origin and low Th/U values has previously been documented (Williams and Claesson, 1987; Keay et al., 2001). Thus, in an attempt to resolve the crystallization age of these three samples, we concentrated on spot analyses (and ages) that more likely represent an igneous origin.

3.2. Sm–Nd analyses

Sm–Nd data (Table 4) were obtained by Van Schmus at the University of Kansas (KU) or by Nelson at the University of Washington (UW) using similar methods. Rock powders for Sm–Nd analysis at KU were dissolved and REE were extracted using the general methods of Patchett and Ruiz (1987). Isotopic compositions for Nd were measured with a VG Sector multicollector mass spectrometer: samarium was
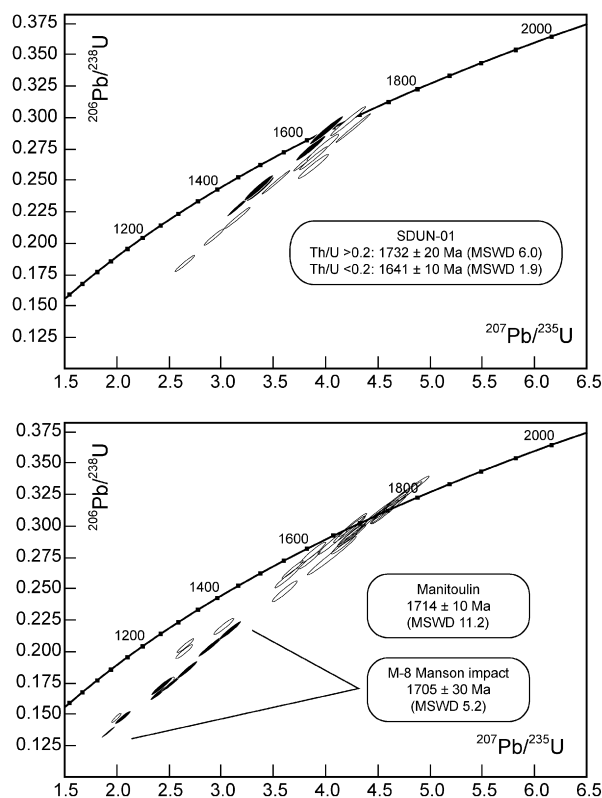

Fig. 4. Concordia plots for SIMS analyses. Upper concordia: SDUN-01 (South Dakota). Lower concordia: Manitoulin Island (ONMI-02) and Manson impact (IA-M8) drill cores. Each ellipse represents a single-spot zircon analysis (2σ). Solid ellipses in upper diagram are data that have Th/U of <0.2 and yield an age of 1641 ± 10 Ma; solid ellipses in lower diagram are from sample IA-M8. See text for further discussion.

loaded with H_3PO_4 on a single Ta filament and typically analyzed as Sm^+ in static-multicollector mode or single-collector mode; neodymium was loaded with phosphoric acid on a single Re filament having a thin layer of AGW-50 resin beads and analyzed as Nd^+ using dynamic-multicollector mode. External precision based on repeated analyses of our internal standard is ±40 ppm (2σ) or better. KU analyses are adjusted for instrumental bias determined by frequent measurements of our intralab Nd standard; this standard was calibrated against the La Jolla Nd standard using an assigned value of 0.511860 for $^{143}Nd/^{144}Nd$ (normalized to $^{146}Nd/^{144}Nd = 0.72190$). Eight analyses of BCR-1 have yielded Nd = 29.44 ± 0.70 ppm, Sm = 6.77 ± 0.21 ppm, $^{147}Sm/^{144}Nd = 0.13931 ± 0.00071$, and $^{143}Nd/^{144}Nd = 0.512641 ± 0.000007$, yielding $\varepsilon_{Nd}(0) = 0.07 ± 0.12$ (all at 1σ). Sm–Nd ratios are correct to within ±0.5%, based on analytical uncertainties; $\varepsilon_{Nd}(t)$ values were calculated using the U–Pb ages defined from zircons where avail-

Table 3

Ion microprobe U–Pb isotopic data

	$\frac{206\text{Pb}*}{238\text{U}}$	$\frac{206\text{Pb}*}{238\text{U}}$ (1s.e.)	$\frac{207\text{Pb}*}{235\text{U}}$	$\frac{207\text{Pb}*}{235\text{U}}$ (1s.e.)	$\frac{207\text{Pb}*}{206\text{Pb}*}$	$\frac{207\text{Pb}*}{206\text{Pb}*}$ (1s.e.)	Th/U	U (ppm)	Th (ppm)	$206\text{Pb}*$ (%)	$207\text{Pb}*$ (%)	Age (Ma) $\frac{206\text{Pb}}{238\text{U}}$	$\frac{206\text{Pb}}{238\text{U}}$ (1s.e.)	$\frac{207\text{Pb}}{235\text{U}}$	$\frac{207\text{Pb}}{235\text{U}}$ (1s.e.)	$\frac{207\text{Pb}}{206\text{Pb}}$	$\frac{207\text{Pb}}{206\text{Pb}}$ (1s.e.)	Correlation of concordia ellipses
ONMI-02																		
L5gr2sp1[a]	0.2973	0.0111	4.2360	0.1607	0.1033	0.0005	0.293	555	191	99.8	98.4	1678.1	55.2	1681.0	31.2	1684.5	8.1	0.99
L5gr1sp1[a]	0.2581	0.0076	3.6230	0.1085	0.1018	0.0006	0.446	792	414	99.4	95.3	1480.2	39.2	1554.6	23.8	1657.1	10.2	0.98
L5gr1sp2[a]	0.2481	0.0080	3.6100	0.1162	0.1055	0.0008	0.290	309	105	98.8	91.5	1428.7	41.1	1551.8	25.6	1723.7	13.7	0.97
L5gr8sp1[a]	0.3045	0.0087	4.4420	0.1251	0.1058	0.0004	0.236	628	174	99.9	99.3	1713.7	42.8	1720.2	23.3	1728.1	6.6	0.99
L5gr10sp1[a]	0.3276	0.0131	4.8020	0.2045	0.1063	0.0008	0.465	320	175	99.9	99.3	1826.6	63.4	1785.3	35.8	1737.3	13.4	0.99
L5gr16sp1[a]	0.2053	0.0054	2.6560	0.0741	0.0938	0.0006	0.220	578	149	99.6	97.0	1203.8	28.9	1316.4	20.6	1504.8	11.1	0.98
L5gr15sp1[a]	0.2731	0.0073	3.8570	0.1024	0.1024	0.0004	0.267	976	306	99.5	96.2	1556.8	36.8	1604.8	21.4	1668.4	7.3	0.99
L5gr18sp1[a]	0.2859	0.0080	4.1830	0.1206	0.1061	0.0008	0.353	219	91	99.9	99.2	1621.2	40.1	1670.7	23.6	1733.4	14.2	0.96
L5gr12sp1[a]	0.3124	0.0100	4.5640	0.1411	0.1059	0.0004	0.504	816	483	99.9	99.6	1752.7	49.1	1742.7	25.8	1730.7	7.1	0.99
L5gr12sp2[a]	0.2950	0.0075	4.2820	0.1085	0.1053	0.0003	0.503	977	577	99.9	99.1	1666.5	37.3	1689.9	20.8	1719.1	6.0	0.99
L1gr1sp1[a]	0.2780	0.0080	3.8850	0.1133	0.1013	0.0007	0.463	312	170	99.9	99.0	1581.5	40.3	1610.5	23.6	1648.7	12.1	0.98
L1gr5sp1[a]	0.3240	0.0126	4.7540	0.1908	0.1064	0.0006	0.378	288	128	100.0	99.7	1809.3	61.1	1776.8	33.7	1738.8	10.6	0.99
L1gr7sp1[a]	0.2004	0.0056	2.6430	0.0758	0.0957	0.0009	0.374	964	423	99.1	93.1	1177.5	30.0	1312.8	21.1	1541.1	17.2	0.95
L1gr8sp1[a]	0.3141	0.0126	4.6200	0.1798	0.1067	0.0007	0.508	183	109	99.9	99.4	1760.8	61.6	1753.0	32.5	1743.7	11.5	0.99
L1gr9sp1[a]	0.2868	0.0098	4.0750	0.1412	0.1030	0.0006	0.448	537	282	99.6	96.9	1625.7	48.9	1649.2	28.3	1679.4	10.3	0.99
L1gr10sp1[a]	0.2648	0.0073	3.6930	0.1026	0.1011	0.0004	0.297	946	330	99.6	96.7	1514.5	37.1	1569.9	22.2	1645.2	7.0	0.99
L1gr11sp1[a]	0.3023	0.0100	4.2660	0.1433	0.1024	0.0004	0.354	597	249	99.6	96.8	1702.6	49.7	1686.9	27.6	1667.4	7.8	0.99
L1gr13sp1[a]	0.1736	0.0043	2.4730	0.0667	0.1033	0.0010	0.411	274	132	99.9	99.6	1031.9	23.8	1264.1	19.5	1684.5	17.8	0.93
L1gr15sp1[a]	0.2943	0.0095	4.2780	0.1377	0.1054	0.0006	0.381	319	143	99.9	99.2	1663.0	47.5	1689.2	26.5	1721.8	9.8	0.99
L1gr16sp1[a]	0.1475	0.0032	1.9990	0.0408	0.0983	0.0005	0.388	503	229	99.6	96.5	886.87	17.8	1115.3	13.8	1592.5	10.0	0.97
L1gr18sp1[a]	0.2934	0.0097	4.2370	0.1415	0.1047	0.0005	0.414	496	241	99.9	99.3	1658.6	48.2	1681.3	27.4	1709.7	8.6	0.99
L1gr20sp2[a]	0.2776	0.0160	4.0570	0.2390	0.1060	0.0007	0.459	223	120	99.9	99.4	1579.3	80.7	1645.7	48.0	1731.6	12.6	0.99
L1gr18sp2[a]	0.3120	0.0089	4.5360	0.1297	0.1054	0.0003	0.666	499	391	99.9	99.1	1750.5	43.8	1737.6	23.8	1722.0	4.6	1.00
L1gr19sp1[a]	0.2193	0.0065	3.0240	0.0916	0.1000	0.0006	0.285	427	143	99.9	99.0	1278.1	34.6	1413.7	23.1	1624.4	10.2	0.98
L1gr12sp1[a]	0.3174	0.0115	4.6500	0.1675	0.1062	0.0008	0.522	157	96	99.8	98.3	1777.2	56.0	1758.2	30.1	1735.7	13.1	0.98
L5gr7sp1	0.2302	0.0087	2.9460	0.1370	0.0928	0.0017	0.180	1336	283	99.5	95.6	1335.3	45.4	1393.8	35.2	1484.6	35.0	0.93
L5gr7sp2	0.2343	0.0056	2.9850	0.0734	0.0924	0.0004	0.116	922	126	99.8	98.3	1356.8	29.1	1403.7	18.7	1475.7	7.6	0.99
L5gr17sp1	0.1889	0.0150	2.4130	0.1925	0.0926	0.0028	0.128	354	53	99.4	94.5	1115.3	81.5	1246.4	57.3	1480.4	57.8	0.93
L5gr11sp1	0.2539	0.0064	3.3970	0.0858	0.0971	0.0005	0.201	558	132	99.9	99.2	1458.3	32.8	1503.8	19.8	1568.5	10.2	0.98
L5gr11sp2	0.2501	0.0066	3.2160	0.0873	0.0933	0.0004	0.114	885	118	99.8	98.4	1439.0	34.2	1461.0	21.0	1493.0	7.3	0.99
L5gr5sp1	0.2535	0.0076	3.3830	0.1035	0.0968	0.0006	0.175	675	139	99.4	94.7	1456.3	39.3	1500.6	24.0	1563.6	10.7	0.98
L5gr4sp2	0.2549	0.0072	3.2540	0.0918	0.0926	0.0004	0.102	928	112	99.9	99.1	1463.5	37.0	1470.2	21.9	1479.8	7.3	0.99
L5gr13sp1	0.2631	0.0076	3.3270	0.0969	0.0917	0.0004	0.083	1175	114	99.7	97.5	1505.9	39.0	1487.5	22.7	1461.4	8.0	0.99
L1gr4sp1	0.2740	0.0097	3.5910	0.1243	0.0951	0.0012	0.133	1186	185	99.8	98.1	1560.8	49.2	1547.5	27.5	1529.4	24.0	0.93
L1gr17sp1	0.2165	0.0055	2.8240	0.0753	0.0946	0.0007	0.112	615	81	98.9	90.8	1263.1	29.4	1361.9	20.0	1520.5	13.5	0.96
L1gr20sp1	0.2176	0.0334	3.0930	0.5018	0.1031	0.0033	0.321	304	114	99.8	98.6	1269.1	177.0	1431.1	124.0	1680.9	59.8	0.98
L5gr4sp1	0.3387	0.0088	4.8150	0.1265	0.1031	0.0005	0.516	356	216	99.9	99.4	1880.2	42.4	1787.6	22.1	1681.1	9.6	0.98
L5gr3sp1	0.3129	0.0073	4.3010	0.1031	0.0997	0.0005	0.779	406	371	99.8	98.5	1754.9	35.7	1693.6	19.8	1618.6	9.2	0.98
L1gr14sp1	0.3054	0.0096	4.2370	0.1366	0.1006	0.0004	0.362	1613	685	99.5	96.2	1718.0	47.3	1681.3	26.5	1635.9	6.5	0.99
L1gr2sp1	0.2504	0.0069	3.3900	0.0962	0.0982	0.0005	0.220	571	148	99.8	98.2	1440.6	35.6	1502.2	22.2	1590.1	10.0	0.98
SDUN-01																		
Ygr3sp1[a]	0.2667	0.0092	3.8930	0.1373	0.1059	0.0006	0.698	229	187	99.9	99.1	1524.2	46.9	1612.3	28.5	1729.4	10.5	0.99
Ygr5sp1[a]	0.1837	0.0067	2.6650	0.0983	0.1052	0.0007	0.468	789	434	99.9	99.5	1087.3	36.2	1318.9	27.2	1718.0	12.6	0.98
Ygr11sp1[a]	0.2195	0.0087	3.1640	0.1311	0.1045	0.0007	0.344	453	183	99.9	99.4	1279.3	46.0	1448.5	32.0	1706.4	12.0	0.99
Ygr11sp2[a]	0.2047	0.0067	2.9440	0.0957	0.1043	0.0009	0.363	433	184	99.9	99.6	1200.7	36.1	1393.4	24.6	1702.0	15.1	0.97
Ygr24sp1[a]	0.2962	0.0117	4.2290	0.1677	0.1035	0.0007	0.243	242	69	99.7	97.7	1672.6	58.0	1679.8	32.6	1688.6	11.7	0.99
Ygr2sp1[a]	0.2758	0.0103	3.9890	0.1525	0.1049	0.0009	0.681	244	195	99.5	96.2	1569.9	51.8	1631.9	31.0	1712.7	15.7	0.97
Ygr1sp1[a]	0.2607	0.0096	3.8980	0.1445	0.1084	0.0008	0.753	264	234	99.8	98.2	1493.5	49.1	1613.3	30.0	1773.4	14.2	0.98
Ygr32sp1[a]	0.2481	0.0095	3.5390	0.1355	0.1034	0.0005	0.368	448	193	99.9	98.9	1428.8	48.8	1535.9	30.3	1686.5	8.4	0.99

Table 3 (*Continued*)

	$\frac{^{206}Pb*}{^{238}U}$	$\frac{^{206}Pb*}{^{238}U}$ (1s.e.)	$\frac{^{207}Pb*}{^{235}U}$	$\frac{^{207}Pb*}{^{235}U}$ (1s.e.)	$\frac{^{207}Pb*}{^{206}Pb*}$	$\frac{^{207}Pb*}{^{206}Pb*}$ (1s.e.)	Th/U	U (ppm)	Th (ppm)	$^{206}Pb*$ (%)	$^{207}Pb*$ (%)	Age (Ma) $\frac{^{206}Pb}{^{238}U}$	$\frac{^{206}Pb}{^{238}U}$ (1s.e.)	$\frac{^{207}Pb}{^{235}U}$	$\frac{^{207}Pb}{^{235}U}$ (1s.e.)	$\frac{^{207}Pb}{^{206}Pb}$	$\frac{^{207}Pb}{^{206}Pb}$ (1s.e.)	Correlation of concordia ellipses
Ygr26sp1[a]	0.2675	0.0108	3.8590	0.1560	0.1046	0.0004	0.447	490	257	99.9	99.1	1528.1	54.8	1605.2	32.6	1707.8	6.4	1.00
Ygr22sp1[a]	0.2912	0.0113	4.2800	0.1659	0.1066	0.0004	0.531	819	511	100	99.7	1647.5	56.4	1689.5	31.9	1741.9	6.4	1.00
Ygr7sp1	0.2292	0.0082	3.1720	0.1142	0.1004	0.0004	0.069	324	26	99.8	98.7	1330.4	43.0	1450.3	27.8	1630.8	7.7	0.99
Ygr30sp1	0.2903	0.0115	4.0170	0.1631	0.1004	0.0005	0.008	267	3	99.8	98.7	1642.9	57.7	1637.7	33.0	1631.0	8.8	0.99
Ygr29sp1	0.2429	0.0097	3.3860	0.1364	0.1011	0.0007	0.047	233	13	99.8	98.6	1401.8	50.1	1501.1	31.6	1644.3	12.2	0.99
Ygr19sp1	0.2442	0.0111	3.3720	0.1552	0.1001	0.0008	0.098	266	31	99.7	97.5	1408.7	57.5	1497.9	36.0	1626.5	15.4	0.98
Ygr12sp1	0.2761	0.0107	3.8820	0.1508	0.1020	0.0006	0.139	284	47	99.8	98.6	1571.6	54.2	1609.8	31.4	1660.2	11.3	0.99
Ygr4sp1	0.3169	0.0150	3.8810	0.1927	0.0888	0.0012	0.220	315	82	97.3	79.4	1774.7	73.2	1609.7	40.1	1400.1	25.1	0.96
Manson M-8																		
Jgr4sp1[a]	0.1726	0.0066	2.4310	0.0940	0.1021	0.0004	0.288	1931	653	99.5	95.8	1026.5	36.5	1251.7	27.8	1663.2	6.40	1.00
Jgr9sp1[a]	0.2038	0.0081	2.8910	0.1164	0.1029	0.0005	0.269	796	252	98.8	91.3	1195.7	43.5	1379.6	30.4	1676.9	9.63	0.99
Jgr19sp1[a]	0.1670	0.0056	2.3950	0.0813	0.1040	0.0006	0.273	953	305	99.3	95.0	995.8	30.9	1241.2	24.3	1696.8	10.60	0.99
Jgr12sp1[a]	0.1474	0.0051	2.0460	0.0726	0.1007	0.0007	0.303	1218	434	98.4	88.3	886.2	28.7	1131.0	24.2	1637.0	13.20	0.98
Jgr13sp1[a]	0.1737	0.0063	2.5010	0.0909	0.1044	0.0005	0.247	1025	297	99.0	92.5	1032.4	34.4	1272.3	26.4	1704.3	8.60	0.99
Jgr17sp1[a]	0.2158	0.0070	3.0640	0.1006	0.1030	0.0003	0.479	2143	1206	99.9	99.2	1259.7	37.3	1423.8	25.1	1678.5	6.23	0.99
Jgr20sp1[a]	0.1362	0.0046	1.9160	0.0646	0.1020	0.0005	0.264	1262	392	99.2	93.5	823.0	26.1	1086.7	22.5	1661.7	9.16	0.99
Jgr19sp2[a]	0.1847	0.0069	2.6550	0.0996	0.1042	0.0005	0.265	1075	335	99.5	96.1	1092.6	37.7	1315.9	27.7	1700.9	8.25	0.99
Jgr14sp1	0.1283	0.0042	1.8620	0.0630	0.1053	0.0008	0.189	1025	227	99.1	93.6	777.9	24.2	1067.8	22.4	1719.6	14.40	0.97
Jgr1sp2	0.1645	0.0059	2.2870	0.0820	0.1008	0.0005	0.178	1998	418	99.1	92.7	982.0	32.5	1208.4	25.3	1639.2	8.30	0.99
Jgr5sp1	0.3577	0.0192	5.4190	0.3268	0.1099	0.0029	0.349	164	66	99.9	99.6	1971.0	91.1	1887.9	51.7	1797.6	48.40	0.90
Jgr8sp1	0.3819	0.0088	5.1640	0.1228	0.0981	0.0011	0.316	325	121	99.6	96.7	2085.2	41.0	1846.7	20.2	1587.2	20.10	0.89
Jgr1sp1	0.1459	0.0051	1.9290	0.0673	0.0959	0.0004	0.244	1956	561	99.6	96.6	878.1	28.5	1091.3	23.3	1545.6	7.61	0.99
Jgr3sp1	0.2132	0.0080	3.1680	0.1195	0.1078	0.0004	0.271	2444	778	99.5	96.3	1245.9	42.3	1449.4	29.1	1762.0	6.63	1.00
Jgr7sp1	0.3966	0.0083	5.3290	0.1049	0.0975	0.0009	0.639	254	191	100	99.8	2153.3	38.4	1873.6	16.8	1576.1	17.10	0.90
Jgr18sp1	0.1453	0.0047	1.9160	0.0620	0.0957	0.0004	0.270	1647	523	99.6	96.6	874.5	26.2	1086.7	21.6	1541.0	7.19	0.99

[a] Grain number, spot number used in determination of U–Pb ages; see text for rationale.

Table 4
Sm/Nd whole-rock results from northern Midcontinent region

Sample (unit name)	Sm (ppm)	Nd (ppm)	$^{147}Sm/^{144}Nd$	$^{143}Nd/^{144}Nd \pm 2\sigma$	$\varepsilon_{Nd}(0)$ (today)	t (Ga)	$\varepsilon_{Nd}(t)$	T_{DM} (Ga)
Iowa drill holes								
2. IACK-01; granite	20.48	130.39	0.0960	0.511622 ± 16	−19.8	1.43	−1.4	1.84
3. IALY-07; keratophyre	7.71	40.44	0.1153	0.511316 ± 09	−25.8	1.78	−7.3	2.70
4. IALY-09; monzodiorite	7.74	63.10	0.0741	0.051040 ± 08	−43.7	2.52	−4.0	2.91
5. IAOS-01; granite	3.81	27.16	0.0859	0.511118 ± 10	−29.6	1.80	−4.0	2.30
Michigan drill hole								
6. MIGT-01A; granite	12.5	65.5	0.1157	0.511815 ± 13	−16.1	1.47	−0.8	1.90
Minnesota drill holes								
7. MNFI-01; metagabbro	4.52	16.86	0.1620	0.512452 ± 08	−3.6	1.76	4.2	1.73
8. MNJK-01; granite	8.33	48.68	0.1035	0.511456 ± 08	−23.0	1.79	−1.6	2.20
9. MNPS-01; metarhyolite cobbles	4.85	27.01	0.1085	0.511567 ± 09	−20.9	1.85	−0.2	2.14
10. MNSH-01; granodiorite gneiss	2.76	17.95	0.0928	0.510531 ± 09	−41.1	*2.80*	−3.7	3.18
Nebraska drill holes								
11. NBBF-01; tonalitic gneiss	4.33	23.28	0.1138	0.511795 ± 12	−16.4	1.79	2.6	1.90
12. NBBU-01; dioritic gneiss	5.50	30.72	0.1094	0.511765 ± 10	−17.0	1.78	2.9	1.87
16. NBKP-01; brecciated granite	12.47	69.34	0.1100	0.511663 ± 10	−19.0	1.78	0.8	2.03
Ontario: Manitoulin Island drill holes								
17. ONMI-01a, 1189′; granite	6.01	42.66	0.0852	0.511274 ± 09	−26.6	1.50	−5.2	2.09
17. ONMI-01b, 1308′; aplite	3.75	32.44	0.0698	0.511163 ± 08	−28.8	1.50	−4.4	1.98
18. ONMI-02a, 2346′; granite gn.	13.33	72.09	0.1118	0.511497 ± 09	−22.3	1.71	−3.6	2.31
18. ONMI-02b, 2391′; migmatite	8.64	44.31	0.1179	0.511660 ± 12	−19.1	1.71	−1.8	2.19
Ontario: Croker Island Complex, North Channel of Lake Huron, outcrop								
24. VS62-13; granite	5.56	42.70	0.0787	0.511248 ± 09	−27.1	1.50	−4.4	2.02
South Dakota drill holes								
19. SDCL-01; granite	10.94	55.97	0.1182	0.511744 ± 08	−17.4	1.76	+1.7	2.08
20. SDDA-01; granodiorite	3.32	20.63	0.0985	0.511123 ± 06	−29.5	1.87	−5.6	2.55
21. SDMO-01; granite	16.89	82.58	0.1250	0.511566 ± 10	−20.9	1.79	−4.3	2.56
22. SDMO-02; rhyolite	10.40	61.24	0.1038	0.511215 ± 18	−27.7	1.83	−6.0	2.55
23. SDUN-01; metagabbro	17.96	75.66	0.1435	0.512040 ± 09	−11.7	1.73	0.15	2.17
Wisconsin, "1760 Ma" granites and rhyolites								
Southern Wisconsin								
25. VS70-01; rhyolite, Berlin	11.83	62.11	0.1152	0.511792 ± 07	−16.5	1.76	1.9	1.94
26. VS70-06; rhyolite, Utley	10.99	55.69	0.1194	0.511864 ± 08	−15.1	1.76	2.4	1.91
27. VS70-07; rhyolite, Marquette	6.57	34.82	0.1141	0.511777 ± 08	−16.8	1.76	1.9	1.94
28. VS70-82; rhyolite, Endeavor	13.36	71.61	0.1129	0.511778 ± 09	−16.8	1.76	2.2	1.91
29. VS70-83; rhyolite, Observatory Hill	15.04	82.20	0.1106	0.511743 ± 07	−17.5	1.76	2.0	1.92
30. VS73-01B; rhyolite, Utley	10.79	56.09	0.1164	0.511803 ± 08	−16.3	1.76	1.9	1.94
Northern Wisconsin (Penokean hosted)								
31. VS73-08; Amberg granite	5.12	30.76	0.1007	0.511555 ± 06	−21.1	1.76	0.6	2.01
32. VS73-37; Radisson granite	12.17	75.25	0.0978	0.511222 ± 05	−27.6	1.78	−5.3	2.41
34. "Sample 23", Monico granite	3.48	16.50	0.1275	0.511858 ± 10	−15.2	1.76	0.0	2.09
Wisconsin, Archean gneiss, eastern part of Marshfield terrane								
33. VS76-37A; migmatite leucosome	1.00	6.40	0.0941	0.510683 ± 11	−38.2	2.78	−1.2	3.02

Notes: See Table 1 for sample location details and sources of U–Pb ages (*t*); Wisconsin "1760 Ma" rhyolite data from B.K. Nelson, University of Washington, adjusted to La Jolla Nd = 0.511860 (nominal value used at Isotope Geochemistry Laboratory, University of Kansas); "Sample 23" from Barovich et al. (1989); all others from W.R. Van Schmus, University of Kansas.

able or estimated ages based on the regional geology and current results from nearby samples. Crustal residence ages (T_{DM}) were calculated following the model of DePaolo (1981a).

Samples run at the UW were also analyzed on a VG Sector, following procedures documented in Nelson (1995). Analysis of La Jolla Nd at UW yielded an average of 0.511840 ± 0.000010. Based on this replica-

tion, and replication of an in-house rock standard ($n = 8$; $2\sigma = 38$ ppm), external precision is ± 40 ppm (2σ). Van Schmus also analyzed the UW in-house rock standard several times and, allowing for normalizing differences relative to La Jolla Nd, obtained equivalent $^{143}Nd/^{144}Nd$ and $^{147}Sm/^{144}Nd$ ratios. In order to have all results on a common datum, $^{143}Nd/^{144}Nd$ ratios reported in Table 4 for UW-analyzed samples (Wisconsin 1.76 Ga rocks) were increased by 0.000020 to account for the difference in nominal values used for $^{143}Nd/^{144}Nd$ in the La Jolla Nd standard. Epsilon values and model ages were recalculated using the model of DePaolo (1981a). The changes from the original UW data that result are slight and commonly within analytical uncertainties, so that interpretations are not significantly affected by them.

3.3. U–Pb and Sm–Nd results

U–Pb data are presented in Tables 2 and 3 and shown in Figs. 1, 3 and 4. Sm–Nd data for samples from the north-central Midcontinent region are summarized in Tables 1 and 4 and Fig. 2. Two key samples are SDUN-01 (McCormick, 2005) and MNFI-01, both of which lie a short distance to the south of the SLtz (Fig. 1). Single-crystal TIMS analyses yield an age of 1733 ± 2 Ma for three analyses from SDUN-01 (Fig. 3A) and 1760 ± 9 Ma for three analyses from MNFI-01 (Fig. 3B). Because of the small sample sizes and the reverse discordance of some of the SDUN-01 data, zircons from this sample were also analyzed by SIMS techniques. Ion microprobe data for SDUN-01 are generally concordant and have lower U contents; the upper intercept for 10 spot analyses on nine zircon grains yields a U–Pb age of 1732 ± 20 Ma, confirming the TIMS age. In addition, zircon data from SDUN-01 with Th/U < 0.2 was plotted separately (Fig. 4), and five spot analyses yield a second age population at 1641 ± 10 Ma. While the younger date is defined by only a few spot ages, it is remarkably similar to the $^{40}Ar/^{39}Ar$ hornblende cooling age from this same sample (1650 ± 2 Ma; see below). We firmly believe that these two separate samples confirm the presence of Yavapai-interval crust adjacent to the Archean craton along the SLtz in Iowa and Minnesota. Sm–Nd model ages (T_{DM}) for these two samples are 2.17 and 1.73 Ga, respectively.

Several other samples confirm this general relationship, although with less precision. A granite from the subsurface in Vermillion, SD (SDCL-01) yielded discordant zircons which give an imprecise age of 1762 ± 28 Ma (Fig. 3C). Geophysical data suggest that this sample lies south of westward continuation of the

Archean margin (SLtz), and a Sm–Nd model age (T_{DM}) of 2.10 Ga (Table 4) supports our interpretation that post-Archean crust occurs at this location. In contrast, zircon from a granite to the north in Davison County, SD (SDDA-01) yields a Penokean (or Trans-Hudson) age of 1871 ± 16 Ma (Fig. 3C); this sample has a T_{DM} age of 2.55 Ga, which clearly indicates a major Archean crustal contribution.

To the east, a drill hole north of the SLtz in Iowa (IAOS-01) yields a U–Pb age of 1804 ± 19 Ma (Fig. 3D) with a T_{DM} age of 2.30 Ga. Similarly, granite sample MNJK-01 in Minnesota yields an age of 1792 ± 31 Ma (Southwick, 1994) with a T_{DM} of 2.20 Ga. Since these two samples lie north of the SLtz, the young (<2.5 Ga) T_{DM} ages suggest that they may be subduction-related with a significant Yavapai-interval mantle component. In contrast, another sample north of the SLtz in NW Iowa, IALY-07 (Table 1), yields an age of 1782 ± 4 Ma with a T_{DM} of 2.70 Ga, indicating derivation primarily from Archean crust. Farther north in Minnesota, a drill core sample of presumed Archean gneiss (MNSH-01) from the eastern part of the Becker Embayment (Fig. 2) yields a Sm–Nd T_{DM} age of 3.18 Ga (Table 4). This model age is compatible with those from the eastern part of the Marshfield Terrane (e.g. VS76-37A, 3.02 Ga, Fig. 2; Table 4), confirming continuation of that terrane into east-central Minnesota (NICE Working Group, 2007).

Farther west, a granite from Keya Paha County in north-central Nebraska (NBKP-01) yields a Yavapai-interval age of 1760 ± 19 Ma (Fig. 3E) with a Sm–Nd model age of 2.03 Ga, providing control for the southern limit of the pre-1800 Ma craton. U–Pb ages for several representative Paleoproterozoic basement samples from Nebraska and Kansas are included in Tables 1 and 2 (Kansas ages from Van Schmus et al., 1993a,b). Two samples, NBBU-01 and NBDA-02, are shown in Fig. 3F; their U–Pb ages of 1771 ± 9 and 1802 ± 4 Ma are clearly in the range of other northern Yavapai terrane rocks. The T_{DM} ages of 1.87 Ga for NBBU-01 and 1.90 Ga for NBBF-01 (Table 4) are also typical of northern Yavapai terrane rocks (DePaolo, 1981b; Nelson and DePaolo, 1985; Ball and Farmer, 1991).

The ca. 65 Ma Manson impact structure in north-central Iowa was drilled as part of an extensive study (Koeberl and Anderson, 1996). Some of the breccia sampled in drill core includes xenoliths of Precambrian basement rock ranging from granite to gneiss. All of these samples are severally altered, with most of the feldspar converted to clay minerals. We obtained one sample of a graphitic granite xenolith at 515 in. depth from drill hole IA-M8 and extracted zircons from it.

SIMS U–Pb data for the zircons from this xenolith are relatively discordant and the grains have generally high U contents (between 1000 and 4000 ppm). The greater discordance for IA-M8 samples compared to analyses for SDUN-01 and MNFI-01 may be a combination of both the higher U contents and thermal/strain disturbance during the impact which produced the Manson structure. In any event, eight spot analyses from seven zircon grains yielded an age of 1705 ± 30 Ma. Although this uncertainty is relatively large, it is clear that none of the zircon have ages >1800 Ma, consistent with our interpretation that geon 17 basement (rather than Penokean basement) occurs throughout northern Iowa.

A major component of the exposed Precambrian basement in Wisconsin south of the proposed SLtz boundary is comprised of the ca. 1.76 Ga granite–rhyolite suite (Smith, 1983). These felsic volcanic rocks and epizonal granite plutons formed 1750 Ma to 1760 Ma (Van Schmus et al., 1975a; Van Schmus, 1978; Holm et al., 2005), but their highly evolved, silicic compositions indicate that they do not represent juvenile orogenic basement. One of us (Nelson) analyzed several of these samples for Sm–Nd; the results are included in Table 4 and shown in Fig. 2. Although the resulting model ages cannot delineate between geon 18 (Penokean) or geon 17 ($\approx$Yavapai) for the age of the crust underlying the rhyolites and epizonal granites south of the SLtz, they clearly indicate an absence of Archean crust and confirm the southerly and easterly limits of the Marshfield terrane.

Projecting the geon 17–geon 16 boundary northeastward is also difficult due to cover from the Michigan Basin. One 1.47 Ga basement sample in Michigan (MIGT-01) yields a Sm–Nd T_{DM} age of 1.9 Ga (Figs. 1 and 2), similar to those in southern Wisconsin. Farther east, two drill holes into Precambrian basement under Manitoulin Island intersected a coarse-grained granite (ONMI-01) and felsic gneiss (ONMI-02). Van Schmus et al. (1975b) determined an age of ca. 1.50 Ga for the granite, indicating that it is a major pluton similar to the Wolf River batholith in Wisconsin. SIMS analyses by two of us (Schneider and Dodson) of zircons from the gneissic sample under Manitoulin Island yielded relatively concordant data, and 25 spot analyses on 20 zircon grains yielded an average U–Pb age of 1714 ± 10 Ma (Fig. 4). Within the cluster of data, several grains suggest that the protolith age for the gneiss could be ca. 1.75 Ga, which is consistent with other data in the region (discussed further below). Sm–Nd T_{DM} ages for samples from these drill holes (Table 4) range from 2.0 to 2.3 Ga, similar to those found

from other Paleoproterozoic basement adjacent to the Superior or Wyoming craton. Another 1500 Ma granite exposed at the surface on North Benjamin Island, north of Manitoulin Island (VS62-13; Van Schmus et al., 1975b), yields a similar Sm–Nd T_{DM} age of 2.02 Ga (Table 4), precluding derivation from Archean crust and indicating that the Archean–Proterozoic boundary must pass between it and the mainland a few km to the north.

3.4. $^{40}Ar/^{39}Ar$ thermochronometry

Hornblende and biotite were separated from basement drill core samples SDUN-01 and MIFI-01 (BO-1) for $^{40}Ar/^{39}Ar$ age spectrum analysis. Size fractions of >150 μm for the target minerals were obtained using standard crushing, heavy liquids, a Frantz magnetic separator, and careful handpicking. Mineral separates were loaded into machined Al discs and irradiated with flux monitor Fish Canyon Tuff sanidine (27.84 Ma; Deino and Potts, 1990) for 100 h in the L-67 position at the 2 MW Ford Reactor at the University of Michigan.

Isotopic analyses were conducted at New Mexico Tech using a MAP 215-50 mass spectrometer on line with an automated all-metal extraction system. The flux monitor crystals were placed in a copper planchet within an ultrahigh vacuum argon extraction system and fused with a 10 W Synrad CO_2 continuous laser. Evolved gases were purified for 2 min using a SAES GP-50 getter operated at $\sim$450 °C. J-Factors were determined to a precision of 0.1% (2σ) by analyzing a minimum of four single-crystal aliquots from each of 3–4 radial positions around the irradiation sample trays. The unknown minerals were step-heated in a double-vacuum Mo resistance furnace; hornblende was heated for 9 min and biotite was heated for 8 min. The gas was scrubbed of reactive species during heating with a SAES GP-50 getter for 6–8 min at 450 °C. Following heating, the sample gas was further cleaned with another GP-50 for 3 min for biotite and 8 min for hornblende. Argon isotopic compositions for both the samples and monitors were determined using the MAP 215-50 mass spectrometer equipped with an electron multiplier with overall sensitivity ranging from 2.66×10^{-16} mol/pA.

Extraction system and mass spectrometer blanks and backgrounds were measured numerous times throughout the course of the analyses. Typical blanks (including mass spectrometer backgrounds) were 1400, 18, 0.3, 2.7, and 4.8×10^{-17} moles at masses 40, 39, 38, 37, and 36, respectively, for furnace temperatures below

1300 °C. Correction factors for interfering nuclear reactions were determined using K-glass and CaF_2 and are as follows: $(^{40}Ar/^{39}Ar)_K = 0.0256 \pm 0.0015$; $(^{36}Ar/^{37}Ar)_{Ca} = 0.00027 \pm 0.00001$; $(^{39}Ar/^{37}Ar)_{Ca} = 0.00070 \pm 0.00005$. All errors are reported at the 2σ confidence level and the decay constants and isotopic abundances are those suggested by Steiger and Jäger (1977). The plateau ages shown represent the integrated ages calculated for the relatively flat portion of each age spectrum (using the concentration of ^{39}Ar to weight both individual ages and errors). This rationale assumes that the steps chosen do not contain excess ^{40}Ar and have not been highly affected by Ar recoil into alteration phases such as chlorite. The calculated plateau age

uncertainties are relatively small because analytical precision in the age of each heating step is high. A plateau age is defined as the part of an age spectrum composed of contiguous increments representing >70% of gas released of which results in concordant ages; a preferred age fails to meet the 70% of ^{39}Ar gas released criterion of a plateau age. The K/Ca plots are determined from Ca-derived ^{37}Ar and K-derived ^{39}Ar, of which the flattest parts of the age spectra generally correspond to relatively constant K/Ca values, whereas younger apparent ages yield relatively high K/Ca values (Marcoline et al., 1999). The age and K/Ca spectra for the samples are presented in Fig. 5 and the analytical results are in Table 5.
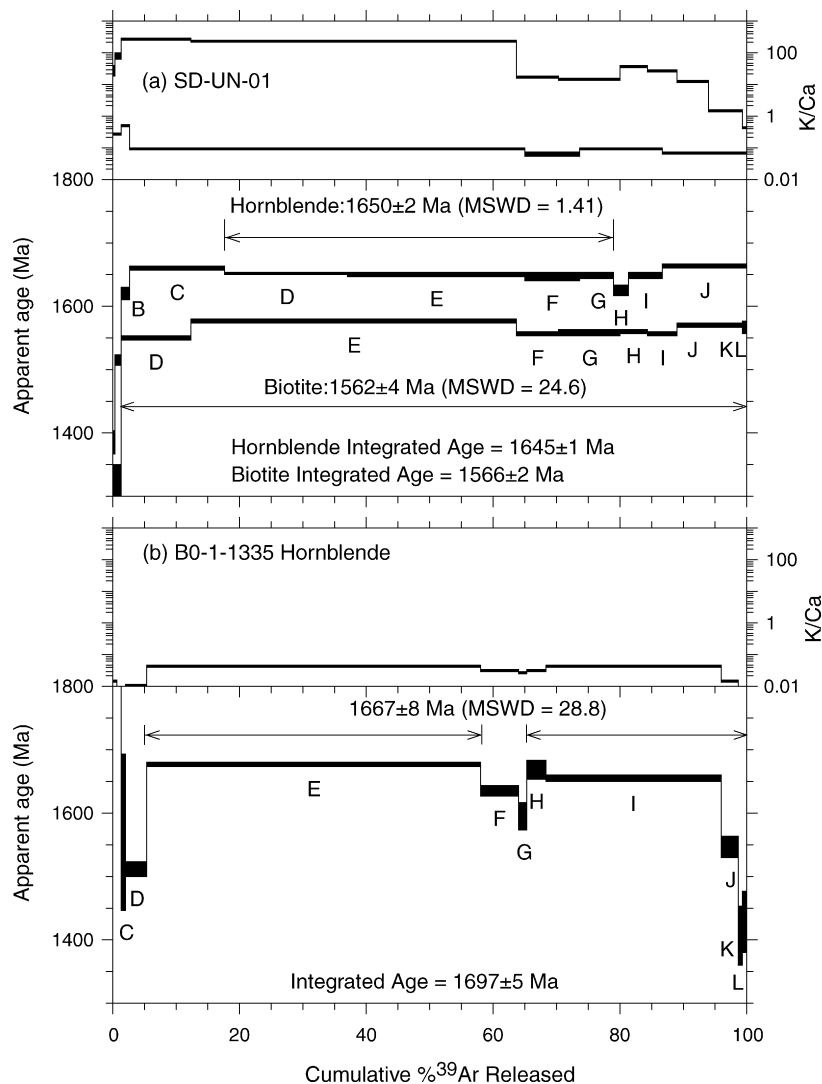
Fig. 5. $^{40}Ar/^{39}Ar$ spectra for hornblende and biotite from SDUN-01, and hornblende from MNFI-01 (MNGS drill hole BO-1). See text for discussion.

Table 5
Ar–Ar data for selected drill hole samples

ID	Temperature (°C)	^{40}Ar/^{39}Ar	^{37}Ar/^{39}Ar	^{36}Ar/^{39}Ar ($\times 10^{-3}$)	^{39}Ar$_K$ ($\times 10^{-15}$ mol)	K/Ca	^{40}Ar* (%)	^{39}Ar (%)	Age (Ma)	$\pm 1\sigma$ (Ma)
SD-UN-01, Biotite, 0.87 mg, $J = 0.01003 \pm 0.22\%$, $D = 1.0055 \pm 0.001$, NM-188H, Lab# 55770-01										
A	550	1159.1	0.0694	3729.5	0.294	7.4	4.9	0.1	816	61
B	650	199.1	0.0175	284.1	0.805	29.1	57.8	0.5	1384.6	8.6
C	720	147.4	0.0060	54.22	2.00	84.5	89.1	1.3	1516.3	4.2
D*	800	137.4	0.0019	5.909	25.8	273.7	98.7	12.4	1549.2	1.6
E*	975	139.4	0.0022	0.4951	119.3	231.1	99.9	63.5	1576.6	2.1
F*	1020	137.1	0.0271	1.459	15.9	18.8	99.7	70.3	1557.2	1.8
G*	1080	137.1	0.0321	0.9519	22.7	15.9	99.8	80.0	1558.2	1.8
H*	1120	137.3	0.0136	1.066	10.1	37.4	99.8	84.4	1559.2	1.9
I*	1160	137.1	0.0186	1.673	10.6	27.5	99.6	88.9	1557.0	2.1
J*	1200	138.8	0.0395	0.9700	11.8	12.9	99.8	94.0	1571.1	1.6
K*	1250	138.7	0.3501	0.8587	12.5	1.5	99.8	99.3	1570.9	1.7
L*	1350	140.5	1.186	8.883	1.55	0.43	98.2	100.0	1568.2	5.0
Integrated age $\pm 1\sigma$				$n = 12$	Sum 233.3	Avg. 13.9 ± 0.0	K$_2$O = 10.3%		1566.3	2.7
Plateau $\pm 1\sigma$	Steps D–L		$n = 9$	MSWD = 24.6	Sum 230.2	Avg. 156.9 ± 105.3	Plateau steps 98.7		1562.3	3.9

ID	Temperature (°C)	^{40}Ar/^{39}Ar	^{37}Ar/^{39}Ar	^{36}Ar/^{39}Ar	^{39}Ar$_K$ ($\times 10^{-3}$)	K/Ca ($\times 10^{-15}$ mol)	^{40}Ar* (%)	^{39}Ar (%)	Age (Ma)	$\pm 1\sigma$ (Ma)
SD-UN-01, Hornblende, 3.38 mg, $J = 0.010073 \pm 0.15\%$, $D = 1.004 \pm 0.001$, NM-188G, Lab# 55769-03										
A	800	299.6	1.819	651.9	0.8	0.28	35.7	1.4	1321	14
B	900	154.1	0.9866	33.31	0.7	0.52	93.7	2.7	1619.7	5.4
C	1000	150.3	5.214	4.892	8.4	0.098	99.3	17.5	1659.5	1.6
D*	1020	148.5	5.433	2.386	10.9	0.094	99.8	36.8	1651.9	1.5
E*	1040	148.1	5.426	1.991	15.9	0.094	99.9	64.9	1649.6	1.5
F*	1060	147.3	7.814	2.350	4.9	0.065	100.0	73.5	1646.3	2.8
G*	1080	147.9	5.289	2.430	3.0	0.096	99.8	78.9	1647.4	2.5
H	1100	145.8	5.102	5.342	1.4	0.100	99.2	81.3	1625.1	3.8
I	1150	148.3	5.491	3.601	3.1	0.093	99.6	86.8	1648.3	2.9
J	1250	150.0	6.512	2.542	7.4	0.078	99.9	99.9	1663.8	1.7
K	1650	219.8	4.922	301.0	0.1	0.10	59.7	100.0	1524	40
Integrated age $\pm 1\sigma$				$n = 11$	Sum 56.7	Avg. 0.091 ± 0.001	K$_2$O = 0.64%		1645.0	1.0
Plateau $\pm 1\sigma$	Steps D–G		$n = 4$	MSWD = 1.41	Sum 34.8	Avg. 0.090 ± 0.015	Plateau steps 61.3		1649.8	2.0
BO-1-1335, Hornblende, 3.74 mg, $J = 0.010046 \pm 0.15\%$, $D = 1.0055 \pm 0.001$, NM-188G, Lab# 55768-01										
A	700	9650.3	34.03	30359.7	0.153	0.015	7.1	0.7	3753	138
B	800	4511.1	55.22	13837.6	0.151	0.009	9.5	1.4	3059	88
C	900	1346.3	60.10	4124.0	0.138	0.008	9.8	2.1	1570	61

Table 5 (*Continued*)

ID	Temperature (°C)	$^{40}Ar/^{39}Ar$	$^{37}Ar/^{39}Ar$	$^{36}Ar/^{39}Ar$ ($\times10^{-3}$)	$^{39}Ar_K$ ($\times10^{-15}$ mol)	K/Ca	$^{40}Ar^*$ (%)	^{39}Ar (%)	Age (Ma)	$\pm1\sigma$ (Ma)
D	1000	154.0	41.24	103.3	0.721	0.012	82.4	5.4	1510.5	5.8
E*	1075	153.4	11.04	9.297	11.3	0.046	98.8	57.9	1677.0	1.9
F	1130	150.3	15.81	21.32	1.33	0.032	96.7	64.1	1634.8	4.3
G	1150	145.9	17.54	25.79	0.300	0.029	95.8	65.5	1594	11
H*	1170	152.4	15.02	12.28	0.577	0.034	98.4	68.2	1668.6	7.3
I*	1190	149.6	11.46	6.885	5.99	0.045	99.3	96.1	1655.6	2.1
J	1220	137.2	33.63	26.38	0.540	0.015	96.3	98.6	1547.3	8.5
K	1250	124.8	162.6	112.1	0.133	0.003	84.0	99.2	1407	23
L	1350	133.8	541.5	342.3	0.166	0.001	57.2	100.0	1428	24
Integrated age $\pm1\sigma$		$n=12$			Sum 21.5	Avg. 0.024 ± 0.000	$K_2O = 0.22\%$		1696.8	4.7
Plateau $\pm1\sigma$	Steps E, H, I	$n=3$		MSWD = 28.8	Sum 17.827	Avg. 0.045 ± 0.007	Plateau steps 83.1		1667.3	7.6

Notes: Isotopic ratios corrected for blank, radioactive decay, and mass discrimination, not corrected for interfering reactions. Errors quoted for individual analyses include analytical error only, without interfering reaction or J uncertainties. Integrated age calculated by summing isotopic measurements of all steps. Integrated age error calculated by quadratically combining errors of isotopic measurements of all steps. Plateau age is inverse-variance-weighted mean of selected steps. Plateau age error is inverse-variance-weighted mean error (Taylor, 1982) times root MSWD where MSWD > 1. Plateau error is weighted error of Taylor (1982). Decay constants and isotopic abundances after Steiger and Jäger (1977). Weight percent K_2O calculated from ^{39}Ar signal, sample weight, and instrument sensitivity. Ages calculated relative to FC-2 Fish Canyon Tuff sanidine interlaboratory standard at 28.02 Ma. Decay constant: λ_K (total) = 5.543×10^{-10} year^{-1}. Correction factors: $(^{39}Ar/^{37}Ar)_{Ca} = 0.00067 \pm 0.00001$; $(^{36}Ar/^{37}Ar)_{Ca} = 0.000274 \pm 0.000002$; $(^{38}Ar/^{37}Ar)_K = 0.0124$; $(^{40}Ar/^{39}Ar)_K = 0.0233 \pm 0.0012$.

Hornblende and biotite from sample SDUN-01 (Fig. 5) yield respectable step-heating results that define meaningful plateau ages. Hornblende steps D–G, representing about 60% of the ^{39}Ar gas released yielded a preferred age of 1650 ± 2 Ma that is only slightly older than the integrated age of 1645 ± 1 Ma and concordant to the U–Pb metamorphic zircon age of 1641 ± 10 Ma reported above. Biotite steps D–L, constituting over 95% of the ^{39}Ar gas released, yielded a well-defined plateau age of 1562 ± 4 Ma that is essentially indistinguishable from the integrated age of 1566 ± 2 Ma. Hornblende separated from drill core sample BO-1 reveals a more complex age spectrum with anomalous initial and final age increments probably due to impurities or alteration. However, three increments (E, H, and I), constituting over 80% of the total ^{39}Ar gas released, yield a meaningful plateau age of 1667 ± 8 Ma.

4. Implications for distribution of Archean and Paleoproterozoic terranes

Below we use new and existing data to delineate the nature and extent of Paleoproterozoic crustal terranes across the North American Midcontinent. Specifically, we focus on formation of geon 17 ($\approx$Yavapai-interval) crust in the northern Midcontinent (south of the Spirit Lake tectonic zone), formation of geon 16 ($\approx$Mazatzal-interval) crust in the central Midcontinent, thermal and deformational overprinting due to geon 16 orogenesis, and correlation of these to the southwest and the northeast.

Because of sparse field and geochronologic control in the Midcontinent region, we obviously cannot correlate to well-documented regions to the east or west on a specific event-by-event basis. Instead, we are using the better exposed and well understood Paleoproterozoic terranes of the southwestern U.S. as a major reference base from which to extrapolate general, first-order relationships. Our discussion is not meant to convey a model whereby large, isochronous Yavapai or Mazatzal superterranes docked along the southern margin of Laurentia, but rather, it recognizes a framework in which several smaller arcs were generated, trapped, and accreted at various times during geon 17 and geon 16, with allowances for limited areal extents of individual sub-terranes and a variety of ages within the broad time-scales of "Yavapai" and "Mazatzal" orogenesis. Finally, we recognize that events within these time frames may have been somewhat time-transgressive from one side of the continent to another.

4.1. Geon 17 (≈Yavapai) crust west of the Mississippi River

The Spirit Lake tectonic zone in the northern Midcontinent and the Cheyenne Belt in the western U.S. both mark the southern limit of Archean and/or Penokean/Trans-Hudson basement in Laurentia. South of these boundaries most, if not all, U–Pb ages obtained up to now are younger than 1800 Ma, with geon 17 ages dominant in the northern Midcontinent (Nebraska, northern Iowa, NW half of Kansas, SE Minnesota, and SE South Dakota) and geon 16 ages pervasive in the central Midcontinent (Missouri, SE half of Kansas and presumably also SE Iowa, although there are no data). Key data relevant to this conclusion are (a) U–Pb zircon data for SDUN-01, MNFI-01 (BO-1), and NBKP-01 which yield crystallization ages of ca. 1730 Ma, ca. 1760 Ma, and ca. 1775 Ma, respectively; (b) ion microprobe analysis of zircons from SDUN-01 which confirm the geon 17 age for that locality; (c) zircon separated from gneissic xenoliths in drill core from the Manson impact structure in Iowa which confirm the existence of geon 17 (but not geon 18) igneous activity; (d) late Paleoproterozoic Sm–Nd T_{DM} ages for these samples (2.17, 1.73, and 2.03 Ga, respectively) which are consistent with other Yavapai terrane model ages (DePaolo, 1981b; Nelson and DePaolo, 1985) and, in particular, with northern Yavapai rocks just south of the Cheyenne Belt (1.88–2.11 Ga; Ball and Farmer, 1991). These data, plus other data from basement south of the SLtz (Tables 1 and 2; Fig. 1), yield no geon 18 (≈Penokean or Trans-Hudson) ages. Thus, all presently available U–Pb data support our interpretation that geon 17 (≈Yavapai) orogenic crust extends eastward from Colorado through Nebraska and into SE South Dakota, northern Iowa, and SE Minnesota (Fig. 1); significant geon 18 (≈Penokean) crust may be entirely absent west of the Mississippi River (see below). Discordant zircons from sample SDCL-01 from Vermillion, SD yield a poorly defined geon 17 age (Fig. 3C) with a T_{DM} age of 2.08 Ga, indicating that the SLtz probably trends just north of Vermillion in this region (Fig. 1).

Several samples in NW Iowa and SW Minnesota yield geon 17 ages, but lie north of the SLtz: IALY-07, IAOS-01, and MNJK-01 (Tables 1 and 2; Fig. 1). Sample IALY-07 overlies rocks yielding Archean U–Pb ages, and it has an Archean T_{DM} age; IAOS-01 and MNJK-01 have intermediate T_{DM} ages of 2.30 and 2.20 Ga, respectively. We suggest that geon 17 magmatism was in part generated beneath Archean crust, perhaps due to north-dipping subduction in this region. Two other samples in South Dakota (SDDA-01, SDMO-02) give geon 18 (Penokean or Trans-Hudson) ages of 1871 ± 16 and 1820 ± 8 Ma with Archean T_{DM} ages of 2.55 and 2.59 Ga, respectively, indicating that geon 18 magmatism within the Archean basement can also be found north of the SLtz.

4.2. Connection (?) of the Spirit Lake tectonic zone with the Cheyenne Belt

There are several issues which make it problematic that the Spirit Lake tectonic zone can be continued westward directly into the Cheyenne Belt. One of these, just mentioned above, is that the Archean basement north of the Spirit Lake tectonic zone in South Dakota, Iowa, and Minnesota was intruded by granitic rocks during both geon 18 and geon 17. Both of these occurrences imply north-dipping subduction under the Superior Province in the northern Midcontinent, first during geon 18 (Penokean or Trans-Hudson) and then during geon 17 (≈Yavapai) terrane convergence. A further implication is that any geon 18 crust originally present in the vicinity of the Spirit Lake tectonic zone has been removed in one way or another (rifting, transcurrent faulting?). These relationships are at variance with those in Wyoming, since geon 18 or geon 17 plutons are absent north of the Cheyenne Belt, and the suture is inferred from this and from geophysical imaging to be south-dipping (cf. Houston et al., 1993; Karlstrom et al., 2005). Thus, there must be some kind of tectonic discontinuity between the Cheyenne Belt and the Spirit Lake tectonic zone.

The Precambrian basement in the central part of North Dakota and South Dakota has major north–south trending geophysical features that continue northward into the exposed Trans-Hudson orogen in Canada (cf. Finn and Sims, 2005). Klasner and King (1986, 1990) and Sims et al. (1993) argued convincingly that these trends represent southward extension of the Trans-Hudson orogen into the north-central United States. Although there are a few geochronological data which support this interpretation, they do not provide precise constraints on the full southward extend of Trans-Hudson orogenic crust. Thus, there is considerable leeway in southern South Dakota with which to provide alternate interpretations for the connection between the Cheyenne Belt and the Spirit Lake tectonic zone. Suffice it to say, that at some point there must be juxtaposition of geon 17 crust against geon 18 crust, whether it be eastward continuation of the Cheyenne Belt, westward continuation of the Spirit Lake tectonic zone (with or without link-up), or some complicated

connection between the two with one or more fault off-sets.

4.3. Eastward continuation of Yavapai crust into Ontario

Archean basement is exposed along the north shore of Lake Huron, underlying Huronian Supergroup metased-imentary rocks. A large ca. 1500 Ma plutonic complex underlies Manitoulin Island in the North Channel of Lake Huron (MI, Fig. 1). This pluton is only known from drill core, but the smaller, coeval Croker Island complex (CI, Fig. 1) is exposed on a group of islands between Manitoulin Island and the mainland (Van Schmus et al., 1975b). New Sm–Nd model ages from granite in the Croker Island complex (VS62-13) and the granite of Manitoulin Island (ONMI-01) yield model ages of ca. 2.0 Ga; gneiss intruded by that granite (ONMI-02) yields model ages of 2.2–2.3 Ga (Table 4). Thus, Archean base-ment does not occur significantly farther south than the north shore of Lake Huron in this area. These data are insufficient, however, to determine if the host to the gran-ites is Huronian, Penokean, or Yavapai.

Zircons from Manitoulin core ONMI-02 yield a SIMS zircon date of 1714 ± 10 Ma (Table 3; Fig. 4). This age is very similar to ages of 1742 ± 1 and 1732 ± 7 Ma (van Breeman and Davidson, 1988) from the Killarney magmatic complex just to the east, along the Grenville Front ("K" in Figs. 1 and 2). There are several other geon 17 plutons on both sides of the Grenville Front tec-tonic zone in this area (Davidson et al., 1992; Davidson and van Breeman, 1994), but geon 18 metamorphic or plutonic ages are absent (Piercey et al., 2007). Thus, these ages argue for continuation of geon 17 basement northeastward to the Grenville Front in Ontario, north of Lake Huron (van Breeman and Davidson, 1988). Crustal studies in the Grenville Province further demonstrate that geon 17 crust continues through Ontario and Que-bec (Barilia) to Labrador (Makkovikia) as recognizable terranes (cf. Rivers, 1997; Dickin, 2000).

Poor exposure and strong overprinting by geon 14 magmatism severely hinders our knowledge of the defor-mational history of Paleoproterozoic crust in the Lake Huron region of Ontario. Historically, the effects of Penokean deformation have been thought to dominate the region. However, recent geochronologic and ther-mochronologic results indicate that a geon 18 overprint is lacking (Piercey et al., 2007). The oldest metamor-phic ages revealed by in situ monazite U–Th–total Pb geochronology are ca. 1800 Ma, with a strong geon 17 and a local geon 14 to geon 15 signature.

4.4. Southern extent of Yavapai crust in the Midcontinent region

A major implication of defining the SLtz as the southern limit of Archean and Penokean-interval crust involves the ca. 1750–1760 Ma granites and rhyolites of central Wisconsin. These rocks (Smith, 1983; Van Schmus, 1978) lie south of the SLtz and, under this inter-pretation, should not be underlain by Penokean-interval crust. This implies that these rhyolites and epizonal gran-ites were derived from partial melting of underlying, newly generated, early geon 17 crust, perhaps due to rapid melting during the development of a 'hot' orogen (Hyndman et al., 2005). Sm–Nd model ages for rocks of this suite (Table 4) yield T_{DM} ages from 1.91 to 1.94 Ga, which is fully compatible with this interpretation (they do not, however, rule out a Penokean-interval component in the magma). A similar younger, possibly analogous, situation occurs in SE Missouri where ca. 1470 Ma granite–rhyolite rocks have T_{DM} ages of 1.47–1.53 Ga and apparently overlie juvenile ca. 1500 Ma basement (Van Schmus et al., 1996).

Yavapai-interval basement rocks are found through-out Nebraska and in two locations in Kansas: NE Kansas (1.78 Ga) and SW Kansas (1.72 Ga), but no geon 17 rocks have been reported from Missouri or southern Iowa. Thus, the southern limit of geon 17 ($\approx$Yavapai) basement probably extends from New Mexico (Jemez lineament; CD-ROM Working Group, 2002; Karlstrom et al., 2005), through SW Kansas to NE Kansas, and northeastward toward southern Lake Michigan. There are few constraints on its exact location, although the NICE Working Group (2007) argues for locating it in southern Wisconsin near the Illinois border. Ter-ranes of geon 16 age also occur within the eastern Grenville Province, notably as "Labradoria" (cf. Rivers, 1997; Dickin, 2000), showing that the geon 17–geon 16 ($\approx$Yavapai–Mazatzal) accretionary couplet was a transcontinental feature.

4.5. Mazatzal deformation and metamorphism in the Midcontinent region

The ca. 1700 Ma Baraboo Interval quartzites which blanket the Penokean and geon 17 ($\approx$Yavapai) terranes of the north-central U.S. were deformed during geon 16 ($\approx$Mazatzal) orogenesis (Holm et al., 1998b). Ther-mochronologic results from the Penokean orogen of northern Wisconsin reveal a greenschist-facies meta-morphic overprint (between 300 and 500 °C) related to arc accretion (Romano et al., 2000; Holm et al., 2007); $^{40}Ar/^{39}Ar$ amphibole ages presented here reveal that a
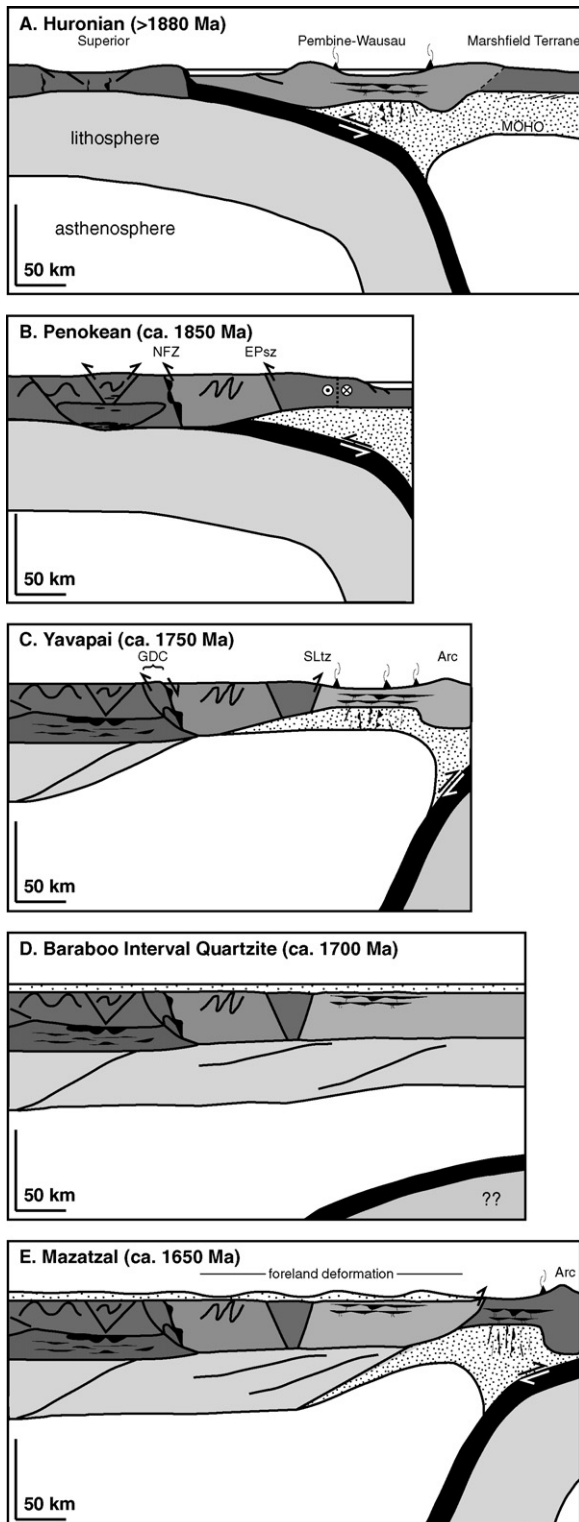
significant region of the geon 17 (≈Yavapai) terrane in Iowa and southern Minnesota was also metamorphosed to amphibolite-facies during geon 16. In contrast, K/Ar ages from Archean basement rocks of the Minnesota River Valley promontory (just north of the SLtz) cluster around 2200–2400 Ma (Goldich, 1968). More recently, Hanley et al. (2006) obtained a ~1615 Ma Ar/Ar age on detrital muscovite from the Sioux quartzite suggesting limited isotopic resetting due to Mazatzal age fluid migration just north of the SLtz. The steep gradient in thermochronologic ages across the SLtz suggests that the Archean crust comprising the promontory was a persistent stronghold in the region that remained largely unaffected by orogenic effects since its formation.

The 1560 Ma biotite cooling age reported here for SDUN-01 is somewhat younger than the cluster of 1575–1615 Ma biotite $^{40}Ar/^{39}Ar$ ages obtained from lower grade Precambrian bedrock in northern Wisconsin (Romano et al., 2000). These biotite ages may represent delayed cooling following Mazatzal metamorphism or partial resetting associated with younger 'anorogenic' melt production.

5. Proposed Paleoproterozoic tectonic evolution

The recognition of a Yavapai-interval terrane in the upper Midcontinent and a corresponding reduction in the southward extent of Penokean-interval crust must be considered in tectonic evolutionary models of the region. Recently, Holm et al. (2005) explained the dominant 1800–1750 Ma magmatism and metamorphic overprint in northern Wisconsin and northern Michigan as being caused by orogenic collapse of overthickened Penokean crust above a north-directed Yavapai-interval subduct-

Fig. 6. Schematic north-south cross-sections depicting the possible Paleoproterozoic accretionary history along the southern margin of Laurentia. (A) Initial Pembine-Wausau arc formation above a newly formed subduction zone and adjacent to the exotic(?) Archean Marshfield terrane. (B) Arc/terrane collision and thrusting along the Niagara Fault zone (NFZ) and Eau Pleine shear zone (EPsz) during the Penokean orogeny, and incipient lateral displacement within the Marshfield terrane along the future Spirit Lake tectonic zone (SLtz). (C) Shortly following subduction flip (Holm et al., 2005), Yavapai convergence facilitated orogenic collapse and formation of the gneiss dome corridor (GDC; Schneider et al., 2004), and generation of juvenile arc crust. (D) Temporary cessation of plate convergence or outboard migration of the trench lead to relative stabilization of localized crustal lithosphere and deposition of the Baraboo Interval quartzites. (E) Renewed subduction, formation of arc crust and ultimate accretion during the Mazatzal orogeny deformed the overlying quartzite units (Holm et al., 1998b) and reheated crust in the southern extent of the region (Romano et al., 2000).

ing lithosphere. In that model, post-Penokean southward growth of Laurentia occurred only by geon 16 terrane accretion of a Mazatzal-interval arc(s). Here, we propose a new history of the tectonic growth and evolution of southern Laurentia based on geochronologic data presented in this paper and on the new terrane map of the upper Midcontinent (Fig. 1).

Penokean arc formation at 1900–1860 Ma (Fig. 6A) and arc or microcontinent accretion ending at ca. 1830 Ma (Fig. 6B) resulted in crustal thickening with foreland deformation and sedimentation along the southern continental margin of Laurentia. The Niagara Fault and Eau Pleine shear zone (Fig. 1) represent paleosutures from this stage. The original volume of juvenile and ancient crust accreted during Penokean orogenesis is not known, although its preservation only within a continental margin embayment (Fig. 1) suggests at least some removal of accreted crust, perhaps by strike-slip translation during margin truncation shortly after Penokean orogenesis. Considerable strike-slip motion along accretionary margins is common and we speculate this process may account for the recent discovery of evidence for latest Archean and geon 18 rocks in central Colorado, south of the Archean Wyoming Province (Hill and Bickford, 2001).

We propose that subduction flip (from south-dipping to north-dipping) following Penokean accretion (Holm et al., 2005) and post-Penokean marginal modification resulted in geon 17 magmatic activity into the Penokean–Archean basement and rapid accretion of geon 17 (≈Yavapai) arc material along the southern Laurentian margin (Fig. 6C) in the Great Lakes region. In this model, suturing occurred along the Spirit Lake tectonic zone simultaneous with exhumation of gneiss dome corridor rocks north of the older Niagara suture (Schneider et al., 2004). Tectonic exhumation in the north was associated with crustal thinning of the over-thickened Penokean crust, whereas accretion to the south accounted for thickening of newly created thin juvenile crust. The end result of geon 17 orogenesis was the creation of young stabilized crust of relative normal thickness. Subsequent, temporary cessation of tectonic activity along the southward growing margin thus set the stage for deposition of ultramature quartz arenites in an area of subdued topographic relief (Fig. 6D; Dott, 1983). The Paleoproterozoic accretionary growth of the north-central Midcontinent culminated with geon 16 (≈Mazatzal) orogenesis (Fig. 6E). The dominant effects of this event are best represented by major south-verging folding in Baraboo Interval quartzites, by emplacement of several geon 16 plutons within geon 17 crust (cf. Fig. 1; Van Schmus et al., 1993a,b), by amphibolite-

facies metamorphism of much of the adjacent geon 17 terrane, and by greenschist-facies metamorphism further north in basement rocks underlying the region of Mazatzal foreland deformation (Holm et al., 1998b).

The presence of geon 16 plutons in Nebraska and Kansas, north of the geon 16–geon 17 boundary (Fig. 1), along with the foreland deformation and metamorphism in Wisconsin, are consistent with north-dipping subduction in the Midcontinent region during geon 16 (Fig. 6E). This is at variance with current models for the Mazatzal–Yavapai boundary in the southwest (cf. Karlstrom et al., 2005), which infer a south-dipping suture, and may indicate a tectonic discontinuity similar to that between the Cheyenne Belt and the Spirit Lake tectonic zone, mentioned above. Geon 16 plutons do occur in Colorado and southern Wyoming, however (e.g. Reed et al., 1993), implying either that subduction polarity was occasionally north-dipping or that there must have been coeval geon 16 extension in the northern (Yavapai) plate. Direct evidence for polarity in the Midcontinent is lacking, and resolution of this problem will have to await further studies. Finally, it should be noted that geon 16 (≈Mazatzal) plutons in the Midcontinent region range to somewhat younger ages than in Arizona and New Mexico. This is probably due in part to variations in timing of orogenic pulses along strike, from Arizona to Labrador, and in part to younging-to-the-southeast variations in the timing of accretionary processes.

Acknowledgments

Chamberlain and Mark Schmitz considerably improved the manuscript.

References

Ball, T.T., Farmer, G.L., 1991. Identification of 2.0–2.4 Ga Nd model age crustal material in the Cheyenne belt, southeastern Wyoming: implications for Proterozoic accretionary tectonics at the southern margin of the Wyoming craton. Geology 19, 360–363.

Barovich, K.M., Patchett, P.J., Peterman, Z.E., Sims, P.K., 1989. Nd isotopes and the origin of 1.9–1.7 Ga Penokean continental crust of the Lake Superior region. Geol. Soc. Am. Bull. 101, 333–338.

Bickford, M.E., Van Schmus, W.R., Zietz, I., 1986. Proterozoic history of the midcontinent region of North America. Geology 14, 296–492.

Bowring, S.A., Van Schmus, W.R., Hoffman, P.F., 1984. U–Pb zircon ages from Athapuscow aulacogen, East Arm of Great Slave Lake, NWT, Canada. Can. J. Earth Sci. 21, 1315–1324.

Bruguier, O., Dada, S., Lancelot, J.R., 1994. Early Archean component (>3.5 Ga) within a 3.05 Ga orthogneiss from northern Nigeria: U–Pb zircon evidence. Earth Planet. Sci. Lett. 125, 89–103.

Catlos, E.J., Gilley, L.D., Harrison, T.M., 2002. Interpretation of monazite ages obtained via in situ analysis. Chem. Geol. 188, 193–215.

CD-ROM Working Group, 2002. Structure and evolution of the lithosphere beneath the Rocky Mountains: initial results from the CD-ROM experiment. GSA Today 12 (3), 4–10.

Davidson, A., van Breeman, O., 1994. U–Pb ages of granites near the Grenville Front, Ontario. Radiogenic Age, Isotopic Studies: Rept. 8. Geological Survey of Canada, Current Research 1994-F, pp. 107–114.

Davidson, A., van Breeman, O., Sullivan, R.W., 1992. Circa 1.75 Ga ages for plutonic rocks of the Southern Province and adjacent Grenville Province: what is the expression of the Penokean orogeny? Radiogenic Age and Isotopic Studies: Rept. 6. Geological Survey of Canada, Paper 92-2, pp. 107–118.

DePaolo, D.J., 1981a. A neodymium and strontium isotopic study of the Mesozoic calc-alkaline granitic batholiths of the Sierra Nevada and Peninsular Ranges, California. J. Geophys. Res. 86, 10470–10488.

DePaolo, D.J., 1981b. Neodymium isotopes in the Colorado Front Range and crust-mantle evolution in the Proterozoic. Nature 291, 193–196.

Deino, A., Potts, R., 1990. Single-crystal ^{40}Ar/^{39}Ar dating of the Olorgesailie Formation, Southern Kenya Rift. J. Geophys. Res. 95, 8453–8470.

Dewane, T.J., Van Schmus, W.R., 2007. U–Pb geochronology of the Wolf River batholith, north-central Wisconsin: evidence for successive magmatism between 1484 Ma and 1470 Ma. Precambrian Res.

Dickin, A.P., 2000. Crustal formation in the Grenville Province: Nd-isotope evidence. Can. J. Earth Sci. 37, 165–181.

Dott Jr., R.H., 1983. The Proterozoic red quartzite enigma in the north central United States: resolved by plate collision? In: Medaris Jr., L.G. (Ed.), Early Proterozoic geology of the Great Lakes region, vol. 160. Geol. Soc. Am. Memoir, pp. 129–141.

Finn, C.A., Sims, P.K., 2005. Signs from the Precambrian: the geologic framework of Rocky Mountain region derived from aeromagnetic data. In: Karlstrom, K.E., Keller, G.R. (Eds.), The Rocky Mountain Region: an evolving lithosphere, vol. 54. American Geophysical Union, Geophysical Monograph, pp. 39–54.

Goldich, S.S., 1968. Geochronology in the Lake Superior region. Can. J. Earth Sci. 5, 715–724.

Hanley, A.J., Kyser, T.K., Hiatt, E.E., Marlatt, J., Foster, S., 2006. The uranium mineralization potential of the Paleoproterozoic Sioux Basin and its relationship to other basins in the southern Lake Superior region. Precambrian Res. 148, 125–144.

Harrison, T.M., McKeegan, K.D., LeFort, P., 1995. Detection of inherited monazite in the Manaslu leucogranite by ^{208}Pb/^{232}Th ion microprobe dating: crystallization age and tectonic significance: Earth Planet. Sci. Lett. 133, 271–282.

Hill, B.M., Bickford, M.E., 2001. Paleoproterozoic rocks of central Colorado: accreted arcs or extended older crust? Geology 29, 1015–1018.

Holm, D.K., Lux, D., 1996. Core complex model proposed for gneiss dome development during collapse of the Paleoproterozoic Penokean orogen, Minnesota. Geology 24, 343–346.

Holm, D.K., Darrah, K.S., Lux, D.R., 1998a. Evidence for widespread ~1760 Ma metamorphism and rapid crustal stabilization of the Early Proterozoic (1870–1820) Penokean orogen, Minnesota. Am. J. Sci. 298, 60–81.

Holm, D.K., Schneider, D., Coath, C.D., 1998b. Age and deformation of early Proterozoic quartzites in the southern Lake Superior region: implications for extent of foreland deformation during final assembly of Laurentia. Geology 26, 907–910.

Holm, D.K., Van Schmus, W.R., MacNeill, L.C., Boerboom, T.J., Schweitzer, D., Schneider, D., 2005. U–Pb zircon geochronology of Paleoproterozoic plutons from the northern mid-continent, USA: evidence for subduction flip and continued convergence after geon 18 Penokean orogenesis. Geol. Soc. Am. Bull. 117, 259–275.

Holm, D.K., Schneider, D.A., Rose, S., Mancuso, C., McKenzie, M., Foland, K.A., Hodges, K.V., 2007. Proterozoic metamorphism and cooling in the southern Lake Superior region, North America, and its bearing on crustal evolution. Precambrian Res. 157, 100–126.

Hoppe, W.J., Montgomery, C.W., Van Schmus, W.R., 1983. Age and significance of Precambrian Basement samples from northern Illinois and adjacent states. J. Geophy. Res. (Red) 88, 7276–7286.

Houston, R.S., et al., 1993. The Wyoming Province. In: Reed, et al. (Eds.), Precambrian: Conterminous U.S., vol. C-2. Geological Society of North America, The Geology of North America, pp. 121–170.

Hyndman, R.D., Currie, C.A., Mazzotti, S.P., 2005. Subduction zone backarcs, mobile belts, and orogenic heat. GSA Today 15, 4–10.

Karlstrom, K., Houston, R., 1984. The Cheyenne belt; analysis of a Proterozoic suture in southern Wyoming. Precambrian Res. 25, 415–446.

Karlstrom, K., Humphreys, E., 1998. Persistent influence of Proterozoic accretionary boundaries in the tectonic evolution of the southwestern North America: interaction of cratonic grain and mantle modification events. Rocky Mt. Geol. 33, 161–180.

Karlstrom, K.E., Whitmeyer, S.J., Dueker, K., Williams, M.L., Bowring, S.A., Levander, A., Humphreys, E.D., Keller, G.R., and the CD-ROM Working Group, 2005. Synthesis of results from the CD-ROM experiment: 4D image of the lithosphere beneath the Rocky Mountains and implications for understanding the evolution of continental lithosphere. In: Karlstrom, K.E., Keller, G.R. (Eds.), The Rocky Mountain Region: An Evolving Lithosphere. Am. Geophys. Union, Geophysical Monograph 54, pp. 421–441.

Keay, S., Lister, G., Buick, I., 2001. The timing of partial melting, Barrovian metamorphism and granite intrusion in the Naxos metamorphic core complex, Cyclades, Aegean Sea, Greece. Tectonophysics 342, 275–312.

Klasner, J.S., King, E.R., 1986. Precambrian basement geology of North and South Dakota. Can. J. Earth Sci. 23, 1083–1102.

Klasner, J.S., King, E.R., 1990. A model for tectonic evolution of the Trans-Hudson orogen in North and South Dakota. In: Lewry, J.F., Stauffer, M.R. (Eds.), The Early Proterozoic Trans-Hudson Orogen of North America. Geological Association of Canada Special Paper 37, pp. 271–285.

Koeberl, C., Anderson, R.R. (Eds.), Manson Impact Structure: Anatomy of an Impact Crater. Geological Society of America Special Paper 302, p. 484.

Krogh, T.E., 1973. A low contamination method for hydrothermal decomposition of zircon and extraction of U and Pb for isotopic age determinations. Geochim. Cosmochim. Acta 37, 485–494.

Krogh, T.E., 1982. Improved accuracy of U–Pb zircon ages by the creation of more concordant systems using an air abrasion technique. Geochim. Cosmochim. Acta 46, 637–649.

Ludwig, K.R., 1988. PBDAT: a computer program for processing Pb–U–Th isotope data, version 1.24. U.S. Geological Survey open-file report 88-542.

Ludwig, K.R., 2001. Isoplot/Ex (rev. 2.49), a geochronological toolkit for Microsoft Excel. Berkeley Geochronology Center Special Publication No. 1a. University of California, Berkeley, p. 55.

Marcoline, J., Heizler, M.T., Goodwin, L.B., Ralser, S., Clark, J., 1999. Thermal, structural, and petrological evidence for 1400 Ma metamorphism and deformation in central New Mexico. Rocky Mtn. Geol. 34, 93–119.

McCormick, K.A., 2005. Drilling of an aeromagnetic anomaly in southeastern South Dakota: results from analysis of Paleozoic and Precambrian core. S.D. Geol. Survey Rept. of Investigations 116, p. 31.

Medaris, G., Singer, B.S., Dott Jr., R.H., Naymark, A., Johnson, C.M., Schott, R.C., 2003. Late Paleoproterozoic climate, tectonics and metamorphism in the southern Lake Superior region and Proto-North America: evidence from Baraboo interval quartzites. J. Geol. 111, 243–257.

Nelson, B.K., 1995. Fluid flow in subduction zones: evidence from Nd- and Sr-isotope variations in metabasalts of the Franciscan Complex, California. Contrib. Miner. Petrol. 119, 247–262.

Nelson, B.K., DePaolo, D.J., 1985. Rapid production of continental crust 1.7–1.9 b.y. ago: Nd isotopic evidence from the basement of the North American mid-continent. Geol. Soc. Am. Bull. 96, 746–754.

NICE Working Group, 2007. Reinterpretation of Paleoproterozoic accretionary boundaries of the north-central United States based on a new aeromagnetic-geologic compilation. Precambrian Res. 157, 71–79.

Paces, J.B., Miller, J.D., 1993. Precise U–Pb age of Duluth Complex and related mafic intrusions, northeastern Minnesota: geochronological insights into physical, petrogenetic, paleomagnetic, and tectonomagmatic processes associated with the 1.1 Ga midcontinent rift system. J. Geophys. Res. 98, 13997–14013.

Parrish, R.R., 1987. An improved micro-capsule for zircon dissolution in U–Pb geochronology. Isotope Geosci. 66, 99–102.

Patchett, P.J., Ruiz, J., 1987. Nd isotopic ages of crust formation and metamorphism in the Precambrian of eastern and southern Mexico. Contrib. Miner. Petrol. 96, 523–528.

Piercey, T., Schneider, D.A., Holm, D.K., 2007. Geochronology of Proterozoic metamorphism in the deformed Southern Province, northern Lake Huron region, Canada. Precambrian Res. 157, 127–143.

Reed Jr., J.C., Bickford, M.E., Tweto, O., 1993. Proterozoic accretionary terranes of Colorado and southern Wyoming. In: Reed, et al. (Eds.), Precambrian: Conterminous U.S., vol. C-2. Geological Society of North America, The Geology of North America, pp. 211–228.

Rivers, T., 1997. Lithotectonic elements of the Grenville Province: review and tectonic implications. Precambrian Res. 86, 117–154.

Rohs, C.R., Van Schmus, W.R., 2006. Isotopic connections between basement rocks exposed in the St. Francois Mountains and the Arbuckle Mountains, southern mid-continent, North America. Int. J. Earth Sci. doi:10.1007/s00531-006-0123-5 (on-line publication, October 25, 2006).

Romano, D., Holm, D., Foland, K., 2000. Determining the extent and nature of Mazatzal-related overprinting of the Penokean orogenic belt in the southern Lake Superior region, north-central USA. Precambrian Res. 104, 25–46.

Schneider, D.A., Holm, D.K., Lux, D., 1996. On the origin of Early Proterozoic gneiss domes and metamorphic nodes, northern Michigan. Can. J. Earth Sci. 33, 1053–1063.

Schneider, D.A., Holm, D.K., O'Boyle, C., Hamilton, M., Jercinovic, M., 2004. In: Whitney, D.L., Teyssier, C., Siddoway, C.S. (Eds.), Paleoproterozoic Development of a Gneiss Dome Corridor in the Southern Lake Superior Region, U.S.A. Gneiss Domes in Orogeny. Geological Society of America Special Paper 380, pp. 339–357.

Shaw, C.A., Heizler, M.T., Karlstrom, K.K., 2005. ^{40}Ar/^{39}Ar thermochronologic record of 1.45–1.35 Ga intracontinental tectonicsm in the southern Rocky Mountains: interplay of conductive and advective heating with intracontinental deformation. In: Karlstrom, K.E., Keller, G.R. (Eds.), The Rocky Mountain Region: An Evolving Lithosphere. Am. Geophy. Union, Geophysical Monograph 54, pp. 163–184.

Sims, P.K., 1990. Precambrian basement map of the northern midcontinent, U.S.A. U.S. Geological Survey Miscellaneous Investigations Map I-1853-A, 1:1,000,000, with pamphlet, p. 9.

Sims, P.K., Peterman, Z.E., 1986. Early Proterozoic Central Plains orogen—a major buried structure in the north-central United States. Geology 14, 488–491.

Sims, P.K., Van Schmus, W.R., Schulz, K.J., Peterman, Z.E., 1989. Tectono-stratigraphic evolution of the Early Proterozoic Wisconsin magmatic terranes of the Penokean Orogen. Can. J. Earth Sci. 26, 2145–2158.

Sims, P.K., et al., 1993. The Lake Superior region and Trans-Hudson orogen. In: Reed, et al. (Eds.), In: Precambrian: Conterminous U.S., vol. C-2. Geological Society of North America, The Geology of North America, pp. 11–120.

Smith, E.I., 1983. Geochemistry and evolution of the early Proterozoic, post-Penokean rhyolites, granites, and related rocks of south-central Wisconsin, U.S.A. In: Medaris Jr., L.G. (Ed.), Early Proterozoic geology of the Great Lakes region, vol. 160. Geol. Soc. Am. Memoir, pp. 113–128.

Southwick, D.L., 1994. Assorted geochronologic studies of Precambrian terranes in Minnesota: a potpourri of timely information. In: Southwick, D.L. (Ed.), Short Contributions to the Geology of Minnesota, 1994. Minnesota Geol. Survey Rept. of Investigations 43, pp. 1–19.

Stacey, J.S., Kramers, J.D., 1975. Approximation of terrestrial lead isotope evolution by a two stage model. Earth Planet. Sci. Lett. 26, 207–251.

Steiger, R.H., Jäger, E., 1977. Subcommission on Geochronology: convention on the use of decay constants in geo- and cosmochronology. Earth Planet. Sci. Lett. 28, 359–362.

Taylor, J.R., 1982. An Introduction to Error Analysis: The Study of Uncertainties in Physical Measurements. Univ. Sci. Books, Mill Valley, California, 270 p.

van Breeman, O., Davidson, A., 1988. Northeast extension of Proterozoic terranes of Mid-Continental North America. Geol. Soc. Am. Bull. 100, 630–638.

Van Schmus, W.R., 1976. Early and middle Proterozoic history of the Great Lakes area, North America. Phil. Trans. R. Soc. Lond., Ser. A280, 605–628.

Van Schmus, W.R., 1978. Geochronology of the southern Wisconsin rhyolites and granites. Geosci. Wisconsin 2, 19–24.

Van Schmus, R., 1980. Chronology of igneous rocks associated with the Penokean orogeny in WI. In: Morey, G.B., Hanson, G.L. (Eds.), Selected Studies of Archean Gneisses and Lower Proterozoic Rocks, Southern Canadian Shield. Geological Society of America Special Paper 182, pp.159–168.

Van Schmus, W.R., Anderson, J.L., 1977. Gneiss and migmatite of Archean age in the Precambrian basement of central Wisconsin. Geology 5, 45–48.

Van Schmus, W.R., Thurman, M.E., Peterman, Z.E., 1975a. Geology and Rb–Sr chronology of Middle Precambrian rocks in eastern and central Wisconsin. Geol. Soc. Am. Bull. 86, 1255–1265.

Van Schmus, W.R., Card, K.D., Harrower, K.L., 1975b. Geology and ages of buried Precambrian rocks, Manitoulin Island, Ontario. Can. J. Earth Sci. 12, 1175–1189.

Van Schmus, W.R., Bickford, M.E., Zietz, I., 1987. Early and Middle Proterozoic provinces in the central United States. In: Kroner, A. (Ed.), Proterozoic Lithospheric Evolution. Am. Geophys. Union Geodynamics Ser. 17, pp. 43–68.

Van Schmus, W.R., Bickford, M.E., Anderson, R.R., Shearer, C.K., Papike, J.J., Nelson, B.K., 1989. Quimby, Iowa scientific drill hole: definition of Precambrian crustal features in northwestern Iowa. Geology 17, 536–539.

Van Schmus, W.R., Bickford, M.E., Sims, P.K., Anderson, R.R., Schearer, C.K., Treves, S.B., 1993a. Proterozoic geology of the western Midcontinent basement. In: Reed, et al. (Eds.), Precambrian: Conterminous U.S., vol. C-2. Geological Society of North America, The Geology of North America, pp. 239–259.

Van Schmus, W.R., Bickford, M.E., Condie, K.C., 1993b. Early Proterozoic crustal evolution. In: Reed, et al. (Eds.), Precambrian: Conterminous U.S., vol. C-2. Geological Society of North America, The Geology of North America, pp. 270–281.

Van Schmus, W.R., Bickford, M.E., Turek, A., 1996. Proterozoic geology of the east-central midcontinent basement. In: van der Pluijm, B.A., Catacosinos, P. (Eds.), Basement and Basins of Eastern North America. Geol. Soc. Am. Special Paper 308, pp. 7–32.

Van Wyck, N., 1995. Oxygen and carbon isotopic constraints on the development of eclogites, Holsnoy, Norway, and major and trace element, common lead, Sm–Nd, and zircon geochronology constraints on petrogenesis and tectonic setting of pre- and Early Proterozoic rocks in Wisconsin. Unpublished PhD Thesis. University of Wisconsin, 288 pp.

Wallin, E.T., Van Schmus, W.R., 1988. Geochronological studies of the Archean–Proterozoic transition, north-central United States. Geol. Soc. Am. Abstr. Prog. 20, 131.

Williams, I.S., Claesson, S., 1987. Isotopic evidence for the Precambrian provenance and Caledonian metamorphism of high grade paragneisses from the Seve Nappes, Scandinavian Caledonides. II. Ion microprobe zircon U–Th–Pb. Contrib. Miner. Petrol. 97, 205–217.

Windom, K.E., Van Schmus, W.R., Seifert, K.E., Wallin, E.T., Anderson, R.R., 1993. Archean and Proterozoic tectono-magmatic activity along the southern margin of the Superior Province in northwestern Iowa, USA. Can. J. Earth Sci. 30, 1275–1285.